8 June 2016

The influence of tree root water uptake on the long term hydrology of a clay fill railway embankment

Briggs K. M., Smethurst J. A., Powrie W. and O'Brien A. S.

Kevin M. Briggs BEng, EngD (*corresponding author)
Lecturer, University of Bath, Bath, UK.
k.m.briggs@bath.ac.uk
01225 386269

Joel A. Smethurst BEng, PhD
Lecturer, Geomechanics Research Group, Faculty of Engineering and the Environment, University of Southampton, Southampton, UK.

William Powrie FREng, MA, MSc, PhD, CEng, FICE
Dean of Engineering and the Environment, University of Southampton, Southampton, UK.

Anthony S. O'Brien BSc, MSc, DIC, CEng, FICE
Divisional Director, Mott MacDonald; Visiting Professor, Geomechanics Research Group, Faculty of Engineering and the Environment, University of Southampton.

Number of words: 5970

Number of Tables: 3

Number of Figures: 15

Abstract

This paper uses a numerical model to investigate the influence of tree root water uptake and tree removal on pore water pressures and the vertical movement of a clay fill railway embankment. Simulated results of soil wetting and drying are compared with field measurements from an instrumented railway embankment before and after tree removal. A parametric study compares the influence of vegetation on the seasonal movement of the embankment slope. The simulations and field measurements show that while trees cause significant seasonal variations in pore water pressure and water content near the soil surface, they can maintain persistent soil suctions at depth within the tree rooting zone. Demonstration of this result using a numerical model requires a root water uptake function that separates spatially the processes of water infiltration, evaporation and transpiration. With all of the trees are removed, the persistent soil suctions established by the trees are lost as water infiltrates from the soil surface. Leaving the trees in place over the bottom third of the slope can maintain persistent suctions at the slope toe, while potentially also reducing seasonal ground movements at the crest that may adversely affect railway track geometry.

Keywords: climate model, embankment, railway, trees, vegetation

Introduction

Trees cover many of the earthworks (embankments and cuttings) that support or flank a large part (>10,000 km) of the UK's railway infrastructure. Dense vegetation, including mature trees, often became established on earthwork slopes when aggressive lineside vegetation management ceased in the 1960's (Gellatley *et al*., 1995). Vegetation provides a natural habitat for wildlife, promoting biodiversity, and a visual and acoustic screen for adjacent residential areas (Glendinning *et al*., 2009). However, the seasonal and persistent influence of trees on water movement within embankment and cutting slopes can have both positive and negative impacts on the performance of earthworks as transport infrastructure assets (Glendinning *et al*., 2009).

Railway embankment slopes are typically less than 10 m high, with low total stresses on potential failure planes, while trees can generate soil suctions of 1500 kPa up to 2-3m depth (Biddle, 1998). Therefore trees can have a significant influence on the effective stress state within a railway embankment and hence on slope stability (O'Brien *et al*, 2004; Greenwood *et al*., 2004; O'Brien, 2013). In over-steep embankments and embankments vulnerable to progressive failure, tree induced suctions may be crucial in preventing deep-seated instability (O'Brien, 2007; Glendinning *et al*, 2009; Loveridge *et al*, 2010).

In temperate climates, the ability of a tree to transpire, remove water from the soil and generate soil suctions varies seasonally. Rainfall and soil water are evaporated from the surface or removed by tree roots during the summer months, when solar radiation is greatest. Transpiration and surface evaporation reduces or ceases during the winter months when solar radiation is reduced, allowing rainfall to infiltrate and wet the soil. This causes cycles of drying and wetting, and associated pore water pressure changes within the soil. In embankments constructed of clay having a high volume change potential, these are accompanied by

corresponding seasonal cycles of soil shrinkage and swelling (Loveridge *et al*, 2010; Smethurst *et al*, 2015), which can result in train speed restrictions leading to delays for passengers, and require expensive re-levelling work (Scott *et al*., 2007; Glendinning *et al*, 2009).

Infrastructure owners must manage slope vegetation, including mature trees, so as to reduce the influence on track movement without compromising embankment stability. Approaches to vegetation management include removing trees from the upper two thirds of the slope (Smethurst *et al*., 2015), or from within a certain distance of the track depending on the tree species and height (Briggs *et al*., 2013b; London Underground Ltd, 2010). However these approaches are based empirically on datasets of less than two years; and the depth and extent of tree influence on the pore water pressures within embankments is poorly understood.

The influence of tree root water uptake on pore water pressures and ground behaviour has been investigated using finite element analyses incorporating root water uptake functions by Feddes *et al*. (1978), Wilkinson *et al.,* (2002), Indraratna, *et al*. (2006), Rees & Ali (2006), Nyambayo & Potts (2010), Fatahi *et al.* (2009), and Fatahi *et al.* (2014), as distinct from the combined evapotranspiration models used to model grass vegetation cover by Allen *et al*. (1994) and Smethurst *et al*. (2006). Analyses incorporating root water uptake functions remove transpired water by means of a volumetric sink term in Richards' (1931) equation, which governs moisture flow in an unsaturated soil (e.g. Equation A8). The simpler of these approaches adopt a linear distribution of root water uptake within the soil, which decreases with both depth and radius from the tree (Rees & Ali, 2006), or with depth alone for one-dimensional conditions (Prasad, 1998; Briggs *et al.,* 2014). Alternatively, where the root distribution, root growth rate and leaf area index (LAI) of a tree is known, the root water uptake function can include the non-linear removal of potentially transpired water based on root length density and annual leaf growth and senescence rates (Fatahi *et al.,* 2009; Fatahi *et al.,* 2014).

This paper presents and uses an unsaturated numerical model incorporating tree root water uptake to investigate the influence of mature tree cover and tree removal on embankment hydrology. Simulation results are compared with field measurements from an extensively instrumented London Clay railway embankment at Hawkwell, Essex (Smethurst *et al*., 2010; Smethurst *et al*., 2015). A parametric analysis is used to explore the influence of vegetation cover on embankment movement, and the limitations of the numerical model are discussed.

Monitoring of tree removal at Hawkwell embankment

The instrumented site is at Hawkwell, on the Shenfield-Southend Victoria line north of Southend, Essex, UK (Figure 1a; OS grid reference TQ856923). The 5.5 m tall embankment was constructed around 1887 from a fill consisting mainly of London Clay excavated from adjacent areas of cut. The clay embankment fill was of intermediate plasticity, containing occasional coarse to fine gravels, small pockets of ash and sand and fragments of brick. The underlying geology is the London Clay Formation, to about 5 m below the original ground surface comprising a stiff, brown-yellow clay of high plasticity (Smethurst *et al*., 2015). The embankment is capped with ash and ballast. The instrumented section of the embankment was densely vegetated with mature and semi-mature oak (*Quercus robur*) and ash (*Fraxinus excelsior*) trees until March 2007, when the trees were removed from the upper two-thirds of the slope (Figure 1b). Further tree clearance occurred in March 2010, leaving just two semi-mature ash trees at the toe of the south facing slope.

Smethurst et al., (2015) reported measured pore water pressures, soil water contents and slope displacements over a five year period from March 2006. Rainfall was measured using a datalogged tipping bucket rain gauge installed on the north slope.

Field monitoring at Hawkwell showed that climate and vegetation effects influenced soil water content, pore water pressures and shrink-swell displacements within the embankment. The mature trees on the embankment slopes were able to generate large soil suctions and a substantial persistent soil moisture deficit, which was maintained below a depth of approximately 2 m during the winter months (Figure 2a). Removal of the mature trees from the upper part of the embankment in March 2007 resulted in the earthwork gradually re-wetting and the loss of the persistent soil moisture deficit that had been created by the trees.

Small plants and saplings (scrub vegetation) became established on the embankment slopes in the three years following tree removal. These caused seasonal cycles of wetting and drying at shallow depth, with the soil drying that occurred during the summer months being reversed during the winter (Figure 2b). Smethurst *et al*. (2015) noted that while pore water pressure profiles within the embankment slopes remained sub-hydrostatic over the period of monitoring following tree removal, the pore water pressures could potentially increase in the future under different weather or vegetation cover scenarios. This could potentially affect the effective stress and hence the stability of the embankment slope.

Simulation of tree removal at Hawkwell embankment

The finite element software Vadose/w (Geo-Slope, 2007a) was used to model Hawkwell embankment (Smethurst *et al*., 2015), and to explore the extent to which a simple root water uptake function and climate boundary condition can reproduce the near surface changes in water content measured. Vadose/w has previously been used to investigate the sensitivity of pore water pressures in railway earthwork slopes to seasonal climate and soil permeability (Loveridge *et al*., 2010; Briggs *et al*., 2013a; Briggs *et al*., 2014).

Vadose/w

Vadose/w (Geo-Slope 2007) calculates coupled water and heat flow in response to a climate boundary condition, using a modified version of Richards' equation (Richards, 1931) for transient flow in saturated and unsaturated soil (Equations A1, A2 & A3). Heat energy transfer associated with condensation and vaporisation is incorporated into the formulation, allowing soil-atmosphere interaction modelling where significant liquid-vapour transformation occurs (Geo-Slope 2007).

The climate boundary condition within Vadose/w applies a net moisture flux to the soil surface in daily timesteps, according to the water balance equation

$$NF_s = R - AE - RO \quad (1)$$

where NF_s is the net moisture flux into the soil surface (mm/m^2), AE is actual evaporation (mm/m^2; Equation A6), R is rainfall (mm/m^2) and RO is runoff (mm/m^2). Rainfall is a model input, while AE and RO are functions of weather and the soil suction at the soil surface. When daily rainfall exceeds daily actual evaporation, an infiltration flux is applied to the soil surface. Water unable to infiltrate into the soil is assumed to run off and is removed from the simulation. Transpired water is removed from within a defined root zone. The surface water balance and root water uptake are shown in Figure 3.

Water abstraction is calculated from user defined Potential Evapotranspiration (PET; Equation A4), both from the soil surface (Equation A6) and from a defined root zone (Equation A7) using a root water uptake function (Equation A9). The root water uptake function acts as a volumetric sink term in the flow equations, allowing either a uniform or a linearly decreasing water extraction rate with depth (Prasad, 1988; Tratch *et al.*, 1995). The transpiration available

for root water uptake is calculated from the evaporation for a bare soil surface, modified by means of an empirical relationship based on the Leaf Area Index (LAI; Ritchie, 1972), which defines the proportion of solar energy intercepted by vegetation cover to drive transpiration (Equations A6 & A7).

The moisture / heat flow and boundary condition equations used in the simulation are summarised in the Appendix.

Finite element model

A two dimensional finite element model of the Hawkwell embankment (Smethurst *et al*., 2015) was created using Vadose/w (Figure 4). The model simulated the clay fill embankment and London Clay foundation, and the ash and ballast at the embankment crest (Figure 4). The mesh comprised 0.1 m deep elements in the surface layer of the embankment slope to enable calculation of the pore water pressure response to the relatively high pore pressure gradients created by the boundary condition. 0.5 m deep elements were used within the remainder of the root water uptake zone, between 1 m and 3m depth; and 1 m square elements below 3 m depth.

Material properties

As a soil dries and desaturates, its hydraulic conductivity decreases (e.g. Burdine, 1953), reducing liquid and vapour flow rates within the soil and restricting rates of evaporation, transpiration and rainfall infiltration (e.g. Fredlund, 2000). Relationships between soil water content and soil suction, and soil water content and hydraulic conductivity, must be obtained experimentally but may for analytical convenience be represented by formulae such as those proposed by van Genuchten (1980) and Mualem (1976) respectively.

The relationship between water content and suction used for the in situ London Clay was based on the soil water retention curve (SWRC) measured for London Clay in drying by Croney

(1977). This was represented by the van Genuchten (1980) curve fit (Figure 5) with the parameters shown in Table 1. The simulated pore water pressures are known to be sensitive to the London Clay wetting or drying SWRC used (Briggs, 2011; O'Brien, 2013). Laboratory measurements on which to base the definition of a SWRC (or series of SWRC's) for the clay fill were not available for Hawkwell embankment. Therefore the SWRC for clay fill was estimated from that for London Clay in drying and compared with in situ measurements of soil suction and volumetric water content (Figure 5). The clay fill was assigned a lower air entry value and a curve of shallower gradient than the in situ London Clay, reflecting its greater specific volume and wider range of pore sizes, following Loveridge *et al.* (2010) and Briggs *et al.* (2013a). A SWRC for fouled ballast (given by Duong *et al*., 2013) was used to model the ash / ballast layer at the site.

For all soil types, the reduction of soil hydraulic conductivity (below the saturated value, k_{sat}) with increasing soil suction was calculated from the SWRCs using the Mualem (1976) method with the van Genuchten (1980) parameters indicated in Table 1 (Figure 6).

Figure 6 shows the saturated permeability, k_{sat} (close to 0 kPa pore suction), used for each soil layer in the finite element model. Loveridge *et al*., (2010) showed that measured values of permeability in old tipped clay fill railway earthworks can vary by orders of magnitude, and are generally an order of magnitude greater than the permeability of in situ clay. The clay fill was assigned $k_{sat} = 5 \times 10^{-8}$ ms^{-1}, which is higher than the measured median value of 3×10^{-8} ms^{-1} for tipped clay fill embankments reported by O'Brien *et al*. (2004). The London Clay foundation soil was assigned $k_{sat} = 5 \times 10^{-9}$ ms^{-1}, consistent with in situ London Clay (Chandler *et al*., 1990; O'Brien *et al*., 2004). The ash and ballast layer was assigned $k_{sat} = 1.75 \times 10^{-5}$ ms^{-1} (Duong *et al*., 2013).

The surface clay fill (up to 1 m depth) was assigned a value of k_{sat} ten times greater in the vertical direction than the clay fill in the core of the embankment (Figure 6, Table 1). This represents the greater permeability of surface soil due to desiccation cracking and fissuring, which facilitates rainfall infiltration (Anderson *et al*., 1982; Li *et al*., 2011, and Glendinning *et al*., 2014, showed that the vertical hydraulic conductivity of a compacted clay fill slope can be up to two orders of magnitude greater at about 0.1 m depth than at 1.0 m depth). Supplementary analysis showed that pore water pressures calculated in the model were insensitive to a similar increase in horizontal conductivity applied to the clay surface.

Figure 5 shows field measurements of soil suction and volumetric water content from closely located piezometer and neutron probe boreholes at the crest of the north facing embankment slope. Laboratory measurements of soil suction on triaxial test samples from tree covered, clay fill embankments (O'Brien *et al*., 2004) are also shown, with volumetric water contents calculated from gravimetric water contents assuming a dry unit weight of 14.6 kN/m^3. The field and laboratory measurements are shown with SWRCs for London Clay and the estimated SWRC for clay fill adopted from Briggs *et al.,* (2013). Figure 5 shows that the field and laboratory measurements lie close to the London Clay and clay fill SWRCs, and are significantly different from the fouled ballast SWRC. However, for a given soil suction up to 90kPa the water content measured in the field is lower than that estimated using the SWRC for clay fill (Figure 5). Therefore by assuming the SWRC for the clay fill shown in Figure 5, a greater soil suction is likely to be calculated in the finite element model than was measured in the field, for a given soil water content. Sensitivity analyses (not shown) using the London Clay wetting or drying SWRCs to model the clay fill (Figure 5) demonstrated that the London Clay wetting curve gave changes in suction and water content that were less responsive to the climate boundary condition than the original simulations using the clay fill SWRC or that carried out with the London Clay drying SWRC. This is because, for a given suction, the water content

(and hence the derived hydraulic conductivity using the Mualem (1976) method) for the London Clay wetting curve is lower than for the drying curve. The calculated pore water pressures during the wetter winter months were less sensitive to the choice of SWRC. It was not possible to fit the simulation results to the monitoring data by adjusting the clay fill SWRC alone.

Boundary conditions

Table 2 summarises the weather and vegetation cover data used to define the climate boundary condition applied at the soil surface. Potential evapotranspiration (PET) was calculated using the Penman-Monteith equation (Equation A4; Allen *et al.*, 1994) and daily values of temperature, relative humidity, wind speed and net solar radiation. These were obtained from a weather station at Shoeburyness in Essex, 11 km from Hawkwell embankment, and from a datalogged tipping bucket rain gauge installed on the north slope of the embankment (Table 3). The orientation of the slopes was ignored, although there will likely be differences in PET between the north and south aspects (e.g. Smethurst *et al.* 2006; Glendinning *et al.* 2014).

More than ten years' weather data were applied to the model, to create an initial pore water pressure condition (2001-2006) and to compare with the field monitoring data (2006-2011). The boundary condition considered only the March 2007 tree clearance (Figure 4); the further tree clearance towards the end of the monitoring period (March 2010) was not modelled.

Water removal from the soil due to evaporation and transpiration was calculated from the daily weather data and distributed at two hour timesteps in a sinusoidal pattern over the hours between sunrise and sunset, which were estimated from the latitude of the Hawkwell site (51.5918° N). The daily rainfall total was assumed to infiltrate into the soil at a uniform rate over twenty four hours. This allowed long term soil wetting and drying in response to seasonal weather patterns and vegetation cover to be considered, but not the short term response to

individual rainfall events. Rainfall interception by the vegetation canopy was not included in the simulated climate boundary condition as in situ interception measurements were not available for the (deciduous) oak and ash trees at the site. A rainfall interception calculation assuming full rainfall interception and a daily canopy storage capacity of 1mm (for an Oak tree in leaf; Rutter & Morton, 1977) between April-October showed that 11-15% of the total annual rainfall used as the input data for the simulations (Table 3) would be intercepted by the canopy. Therefore the rainfall at the soil surface is likely to be greater in the simulation than that received in situ, particularly when the trees are in leaf during the summer.

The plant root depth was used to differentiate between slope vegetation cover types (Table 2). The depth of root water uptake was based on the in situ, long-term patterns of seasonal wetting and drying shown in soil water content profiles in vegetated soils (Biddle, 1998; Smethurst *et al*., 2006; Smethurst *et al*., 2015). It is therefore a measure of the in situ plant drying depth, rather than the actual root biomass (Leung *et al*., 2015) or average root length of roots excavated from the site (Garg *et al.,* 2015). The deep desiccating influence of the mature trees at the site (and as measured by others, e.g. Biddle, (1998)) was represented by a root depth of 3 m. A root depth of 0.2 m was adopted following tree removal, modelling the immature tree and scrub vegetation that remained on the embankment slope. For all slope vegetation conditions a one-dimensional, linear distribution of root water uptake was assumed within the soil; decreasing only with depth (Prasad, 1998; Briggs *et al.,* 2014) and not considering the influence of individual trees and plants (Rees & Ali, 2006; Fatahi *et al.,* 2009; Fatahi *et al.,* 2014) because these were too numerous. No vegetation was associated with the ballasted area beneath the railway track, resulting in surface evaporation only from this region.

Observations made during visits to the Hawkwell site showed leaf coverage of most of the embankment slopes both when the slopes were vegetated by trees and by scrub. Full vegetation

cover and LAI were assumed throughout the year for all vegetation types, allowing the seasonally variable solar energy to drive transpiration rather than surface evaporation, resulting in the removal of water over the full plant root depth (Equations A6 & A7). The model was not sensitive to a reduction of the LAI during the winter months (simulating annual autumn leaf fall in deciduous trees), because solar radiation and hence transpiration were minimal during this period in any case.

In the Vadose/w simulation, the reduction in transpiration due to soil drying is related to the soil suction (kPa) rather than to the volumetric water content, using the relationship proposed by Feddes *et al.,* (1978) and adopted in studies of tree root water uptake by Indraratna, *et al*., (2006), Rees & Ali, (2006) and Fatahi *et al.,* (2014). This reduces root water uptake linearly from its maximum rate between a point (Ψ_l) at 100 kPa suction and zero at the plant wilting point (Ψ_w) at 1500 kPa suction (Figure 7). Root water uptake is also reduced to zero at pore pressures above the anaerobiosis point (Ψ_{an}) – taken as 0 kPa in the model – at which aeration conditions are deficient and root growth is inhibited.

The side and base boundaries of the finite element model were located so as not to influence flow within the embankment slopes and were assumed to be impermeable, with the water table allowed to fluctuate vertically. This represents a transient situation in which the water balance involves water storage within the soil, driven by surface infiltration and evapotranspiration (Freeze, 1969). A potential seepage face was applied to the soil surface on either side of the embankment, which allowed water to flow out of the soil if positive pore pressures developed. An initial distribution of hydrostatic pore water pressure, above and below a zero pressure line 6 m below the soil surface on the south side of the embankment, was defined within the model (Figure 4). The simulated pore water pressure at the beginning of the monitoring period (2006),

following the application of five years of weather data (2001-2006), was found to be insensitive to an initial zero pore water pressure line within +/- 6 m of that shown in Figure 4.

Linking simulated water content to embankment displacement

It is possible to obtain daily nodal pore water pressure and volumetric water content values from the finite element model. The total soil water storage (mm/m^2), over a depth H (mm) was calculated at weekly intervals from the sum of the simulated nodal volumetric water content (θ_i) for n nodes of vertical spacing h_i (mm):

$$Soil\ water\ storage = \sum_{i}^{n} h_i\,(\theta_i) \qquad (2)$$

The depth (H) was assumed to extend from the soil surface to 3 m depth. The vertical movement of the soil at weekly intervals was calculated for the clay fill layer by assuming isotropic shrinkage and swelling in response to the change in soil water storage (Driscoll, 1983). Soil volume change was assumed to occur in the normal range, hence desaturation of the soil in both the structural and residual phases of soil drying was ignored (Biddle, 1998).

Additional simulations with varying root depths were used to assess the impact of alternative slope vegetation cover scenarios on the vertical movement of the embankment. In addition to the tree removal scenario (Table 2), further simulations considered a) tree covered and b) scrub vegetation covered slopes. The tree covered slope (January 2001 to April 2011) had a root depth of 3 m, and the scrub vegetation covered slope model (January 2001 to April 2011) had a root depth of 0.2 m. All other parameters and model inputs remained unchanged from the initial simulation.

Results

The finite element simulations show that trees that extract water from deep within the root system are able to develop a persistent soil moisture deficit within their rooting zone. The persistent soil moisture deficit is maintained only when the depth of root water uptake is greater than the depth of surface water infiltration over a winter period; if the depth of the root zone is less than that of surface water infiltration, the moisture deficit is lost. The depth of surface water infiltration is influenced by the initial soil suction within the tree root zone, the hydraulic conductivity of the soil and the rate and duration of rainfall events. Demonstration of this result requires a root water uptake function that separates, spatially, the removal of transpired water at depth from rainfall infiltration at the soil surface (Figure 3).

Figure 8 shows the cumulative rainfall (R), potential evapotranspiration (PET), actual evaporation (AE) and actual transpiration (AT) calculated at the climate boundary of the finite element model, for the tree removal scenario. Prior to tree removal, the combined AE and AT were very similar to the annual total rainfall, aided by the drier years in 2003, 2004 and 2005. After tree removal in March 2007 the combined AE and AT are slightly lower, but very similar to the levels prior to tree removal.

Additional (not reported) simulations of root depth influence on R, PET, AE and AT showed that the root depth (0.2m, 0.5m, 1m and 3m) did not influence annual AE/AT totals except on two occasions, during particularly dry summer and autumn periods when cumulative rainfall was significantly less than cumulative PET (July- September 2003 and 2009). This confirmed that the changes in pore water pressures due to tree removal (shown in the next section) are the result of the reduced depth of the modelled root zone, rather than its effect on AE/AT totals.

Pore water pressures

Figure 9 shows contours of pore water pressure within the embankment before tree removal, calculated in the finite element simulation. Figure 9 shows that when trees covered the embankment slopes in March 2007, suctions greater than 200 kPa (shown hatched) were still being maintained within the tree root zone (to 3 m depth), despite the preceding wet winter.

Figure 10a shows the calculated pore water pressures at discrete points between 1 m and 4.5 m depth, at the middle of the south facing embankment slope. This shows that root water uptake influenced pore water pressure variation within the tree root zone (up to 3 m depth). Large seasonal variations in pore water pressure occurred within the soil up to 1 m depth prior to tree removal, in response to seasonal weather changes at the soil surface. Deeper within the root zone, a persistent soil suction close to 1500 kPa was maintained at 2 m depth. Following tree removal, the pore water pressures within the clay fill increased towards 0 kPa and the magnitude of seasonal pore water pressure variation was reduced.

Figure 10b compares calculated pore water pressures and field measurements at the crest of the north facing embankment slope, where 1.1 m of ash and ballast overlies the clay fill. Both the field measurements and the simulation showed that pore water pressures increased from negative to positive in response to tree removal. However, while the field measurements show a sharp pore water pressure increase, indicating a wetting front infiltrating from the soil surface, the finite element model showed a gradual pore water pressure increase over a one to two year period. The rapid water infiltration shown by the field measurements in Figure 10b is likely to have occurred through large voids in the ballast and macropores or preferential flow pathways created by the tree roots within the clay fill. This is not well represented by single porosity continuum flow with the hydraulic conductivity functions (Figure 6) for the ash and ballast and clay fill soil layers used in the finite element model. Both the field measurements and the finite

element simulations show seasonal pore water pressure variation, with reasonable agreement from January 2010 - almost three years after tree removal.

Figure 11 shows contours of pore water pressure within the embankment one year (Figure 11a) and four years (Figure 11b) after tree removal, calculated using the finite element model. This indicates that the removal of trees from the upper two thirds of the embankment slopes caused pore water pressures to increase, and the residual suctions previously maintained by the trees at the end of winter (March) to be lost. A zone of residual suction remained in the clay fill below the tree covered area at the toe of the south embankment slope, but not in the clay fill over the upper two thirds of the slope. Residual suctions were not maintained at the toe of the north embankment slope, where ash and ballast covering the slope (Figure 4) facilitated water infiltration and downslope flow during the winter period.

The pore water suctions in the root zone calculated using the finite element model are much larger than those measured at Hawkwell and exceed the measurement capacity (90 kPa suction) of the piezometers installed (Ridley *et al*., 2003). The finite element model assumes that pore water pressures and volumetric water contents are defined by a single drying SWRC, and may overestimate the magnitude of soil suction created by tree root water uptake (Figure 6). Nonetheless the model, in situ and laboratory measurements consistently confirm that large soil suctions can be generated close to mature trees.

With trees present on the side slopes, the model calculates small suctions (<50 kPa) in the soil below the top (horizontal) surface of the embankment (Figure 9). This is consistent with the evaporation-only boundary condition applied at the top of the embankment, which creates a shallow drying zone that is rapidly re-wetted by infiltrating rainfall. Glendinning *et al.* (2014) suggest that pore water pressures in the core of the embankment may be dependent on the nature of the ballast capping and its interface with the clay.

Patterns of soil wetting and drying

Figure 12a shows simulated patterns of wetting and drying at the middle of the south facing embankment slope in 2006 and 2007, prior to tree removal. During the summer months (April to July 2006), the soil dried within the tree root zone and at the soil surface. During the winter months (September 2006 to February 2007), when transpiration and evaporation were reduced, water infiltrated into the soil surface and the volumetric water content increased. However, infiltration did not penetrate to the full depth of the tree root zone during the winter of 2006/2007, allowing a persistent soil moisture deficit to remain below 1 m depth. This is in agreement with the field measurements at Hawkwell (Figure 2a), and patterns of tree root water uptake observed by others (Biddle, 1998).

Figure 12b shows the simulated patterns of wetting and drying at the middle of the south facing slope during the winter of 2010/2011, nearly four years after tree removal. Volumetric water contents reduced to below 40% over a depth of 1 m during June 2010. However, the volumetric water content beneath 1 m depth (in June 2010) was closer to saturation than prior to tree removal in June 2006 (Figure 12a), creating a wetter initial condition for the winter months. An increase in the volumetric water content causes the hydraulic conductivity of the soil to rise (Figure 6), and brings the soil closer to saturation. Thus surface water was able to infiltrate to the full extent of the original tree root zone (3 m depth) during the winter of 2010/2011, bringing it close to saturation in February 2011. This is in agreement with the pattern of wetting shown by the field monitoring data, with the soil coming close to saturation at shallow depths (Figure 2b).

Figure 13 compares profiles of volumetric water content with depth at the end of winter (March), before (2007) and after (2011) tree removal, calculated using the finite element model. Profiles of volumetric water content with depth measured by Smethurst *et al.,* (2015)

are shown for comparison. The profiles show that a persistent soil moisture deficit was maintained below 1.75 m depth throughout the winter of 2006/2007 prior to tree removal. Four years after tree removal (March 2011), the volumetric water content had increased and the persistent soil moisture deficit had been lost.

Figure 14 shows the volumetric water contents and pore water pressures calculated at the tree covered toe of the south facing slope using the finite element model. The mature tree vegetation cover remained in place at this location throughout the period of the study. A persistent soil moisture deficit and soil suctions were maintained within the tree root zone, below a seasonally affected depth. A saturated wetting front (47% volumetric water content) infiltrated from the soil surface to a depth of approximately 1 m by March 2007. This followed a period of rainfall above the long term average (Smethurst *et al.,* 2015); nonetheless the saturated wetting front at the toe of the south facing slope did not infiltrate to and increase pore water pressures over the full tree root depth.

Vertical movement of the embankment

Figure 15 shows the vertical movement at the south midslope calculated for the simulations of tree removal and the alternative (tree and shrub) vegetation cover scenarios. The movements are shown relative to zero displacement on 2 May 2006, and are compared with extensometer measurements at 1.09 m depth (Smethurst *et al.,* 2015). The vertical movements were calculated for the clay fill between 0 m and 3 m depth and therefore include changes in soil water content and the associated volume change between 0 m and 1.09 m depth, which was not measured by the extensometer at Hawkwell.

The tree and scrub vegetation scenarios show seasonal shrinkage and swelling of the clay fill, with larger movements in the tree covered scenario than in the scrub vegetation scenario, particularly during the dry summers of 2006, 2009 and 2010. Both the extensometer

measurements and the tree removal scenario simulation show heave of the clay fill with seasonal shrink-swell cycles of reducing magnitude. Extended analyses (not shown) indicated that heave of the clay fill in the tree removal model continued until April 2013, six years after tree removal, before seasonal shrink-swell displacements reduced to those of the scrub vegetation scenario simulation.

Implications for practice

The removal of deep rooted trees from an embankment slope may reduce tree induced volume change in high plasticity clay soils, hence seasonal track movement. However, a sustained period of soil heave is then likely to occur. Pore water pressures within the embankment will increase, and the contribution of soil suction to slope stability will be lost. Leaving trees on the lower third of an embankment slope makes it more likely that residual suctions will remain within the soil at this location during periods of wet weather. In extremely wet winters, such as 2000/2001 and 2013/2014, the likelihood of soil saturation, raised pore water pressures and hence embankment distress will inevitably increase (Briggs *et al*., 2013a). Nonetheless, in what is essentially a probabilistic design (i.e. based on the probability of a particular set of pore water pressures being exceeded over the design life of the earthwork) retaining the trees over the bottom part of the slope will increase the return period of the wet weather pattern leading to possible embankment instability.

Implications for modelling clay fill embankments

The tree root water uptake simulations representing the water balance and the physical processes of soil wetting and drying from within the tree root zone showed broad agreement with measurements of soil water content at Hawkwell embankment. However, while water

content variation within the finite element model compared well with field measurements, the quantitative simulation of pore water pressures was more difficult. Large soil suctions were generated in the model (up to the plant wilting point of 1500 kPa; Figure 7), which significantly exceeded any of the soil suctions (up to 90 kPa) measured within the embankment. This may have been due to the use in the model of SWRC curves and hydraulic conductivity functions that were not fully representative of the in situ materials. The lack of reliable, site and materials specific data is a pervasive problem in modelling boundary value problems of this type (e.g. Rees & Ali, 2006; Fatahi *et al.,* 2009; Fatahi *et al.,* 2014). The calculated pore water pressures are sensitive to the SWRC curve but there is limited data showing the water retention behaviour of poorly compacted clay fill materials, particularly near the soil surface. Similarly, more field measurements adjacent to individual trees are required to confirm the magnitude and distribution of in situ suctions.

The hydraulic conductivity of an unsaturated soil with large voids, such as railway ballast or cracked and fissured clay, is much greater during the wetting phase than the continuum Van Genuchten-Mualem relationship implies. This means that the observed rapid re-wetting of the soil in response to rainfall infiltration events was not replicated in the finite element model. Better characterisation of two phase water flow and hysteretic water storage, based on experimental data, is therefore required for improved models of wetting and drying in discontinuous media.

Conclusions

1. The removal of soil water from within the root zone is spatially separate from surface evaporation and rainfall infiltration. This allows vegetation such as mature trees with deep root systems to develop persistent soil suctions at depth, which can be maintained in the long term

throughout periods of wet winter weather. The magnitudes of tree induced soil suctions (>90kPa) are sufficient to increase significantly the effective stresses within an embankment slope, and hence improve its stability.

2. Simulations and field measurements showed that tree covered embankment slopes are subjected to seasonal cycles of wetting and drying at the soil surface (to approximately 1 m depth), while persistent soil moisture deficits are maintained at greater depth within the tree root zone (up to 3 m depth) over timescales of years and decades. Demonstration of this result in numerical simulations requires a root water uptake function to separate, spatially, the removal of transpired water at depth from soil-atmosphere interactions at the ground surface.

3. Simulations and field measurements showed that if trees are removed from the embankment slopes, the persistent suctions and soil moisture deficits within the tree root zone gradually dissipate as water infiltrates from the soil surface. Shallow rooted vegetation (<0.2 m root depth) is unable to re-establish persistent soil suctions at depth following tree removal.

4. The simulations show that retaining trees over the lower 1/3 of the slope can maintain persistent suctions within the soil at the slope toe, while reducing the magnitude of pore water pressure variation and soil displacement at the middle and crest of the slope. This distribution of pore water pressures can help maintain some pore suction related benefit to slope stability during the winter, while still significantly reducing seasonal shrinkage and swelling movements at the embankment crest.

5. The applied climate boundary condition incorporating a root water uptake function was able to simulate observed patterns of soil wetting and drying within an embankment before and after tree removal, but limitations to the quantitative simulation of pore water pressures remain. Further field and laboratory measurements are required to characterise root water abstraction and soil water flow in unsaturated, discontinuous soils such as cracked clay and railway ballast.

Acknowledgements

The measurements at Hawkwell embankment were funded by Network Rail and carried out by Geo-Observations Ltd and the University of Southampton. The work was supported by the University of Southampton Industry Doctoral Training Centre (IDTC) in Transport and the Environment (EPSRC grant number EP/G36896/1), and Mott MacDonald. The weather input data supporting this study are openly available from the University of Southampton repository at http://dx.doi.org/10.5258/SOTON/xxxxx.

References

Allen, R. K., Smith, M., Perrier, A., & Pereira, L. S. (1994). An update for the calculation of Reference Evapotranspiration. *ICID Bulletin*, 43(2),35-92.

Anderson, M.G., Hubbard, M.G. and Kneale, P.E. (1982). The influence of shrinkage cracks on pore-water pressures within a clay embankment. *Quarterly Journal of Engineering Geology*, 15, 9–14.

Banks, D. (2012). *An introduction to thermogeology: ground source heating and cooling*. John Wiley & Sons.

Banks, D., Withers, J. G., Cashmore, G., & Dimelow, C. (2013). An overview of the results of 61 in situ thermal response tests in the UK. *Quarterly Journal of Engineering Geology and Hydrogeology*, 46(3), 281-291.

Bell, F. G. (1992). *Engineering properties of soils and rocks* (No. Ed. 3). Butterworth-Heinemann Ltd.

Biddle, P. G. (1998). *Tree root damage to buildings*. Wantage: Willowmead Publishing.

Briggs, K. M. (2011). *Impacts of climate and vegetation on railway embankment hydrology* (Doctoral dissertation, University of Southampton).

Briggs, K. M., Smethurst, J. A., Powrie, W. & O'Brien, A. S. (2013a). Wet winter pore pressures in railway embankments. *Proceedings of the Institution of Civil Engineers – Geotechnical Engineering.* 166 (5), pp. 451-465.

Briggs, K.M., Smethurst, J.A., Powrie, W., O'Brien, A.S. and Butcher, D. (2013b) Managing tree removal from railway earthwork slopes. *Ecological Engineering* 61, (Part C), 690-696. (doi:10.1016/j.ecoleng.2012.12.076).

Briggs, K., Smethurst, J., & Powrie, W. (2014). Modelling the Influence of Tree Removal on Embankment Slope Hydrology. In *Landslide Science for a Safer Geoenvironment* (pp. 241-246). Springer International Publishing.

Burdine, N. T. (1953). Relative permeability calculation from size distribution data, *Trans. AIME*, 198, 71-78.

Chandler, R.J., Leroueil, S. and Trenter, N.A. (1990). Measurements of the permeability of London Clay using a self-boring permeameter, *Géotechnique* 40 (1), 113-124.

Croney, D. (1977), *The design and performance of road pavements*, Technical report, Her Majesty's Stationary Office.

Driscoll, R. (1983). The influence of vegetation on the swelling and shrinking of clay soils in Britain. *Geotechnique*, 33(2), 93-105.

Duong T.V., Trinh V.N., Cui Y.-J., Tang A.M., and Calon N. (2013). Development of a Large-Scale Infiltration Column for Studying the Hydraulic Conductivity of Unsaturated Fouled Ballast. *Geotechnical Testing Journal*, 36(1): 1–10.

Fatahi, B., Khabbaz, H., & Indraratna, B. (2009). Parametric studies on bioengineering effects of tree root-based suction on ground behaviour. *Ecological Engineering*, 35(10), 1415-1426.

Fatahi, B., Khabbaz, H., & Indraratna, B. (2014). Modelling of unsaturated ground behaviour influenced by vegetation transpiration. *Geomechanics and Geoengineering*, 9(3), 187-207.

Feddes, R. A., Kowaklik, P. J., & Zaradny, H. (1978). *Simulation of Field Water Use and Crop Yield*. John Wiley and Sons.

Fredlund, D. G. (2000). The 1999 R.M. Hardy lecture: The implementation of unsaturated soil mechanics into geotechnical engineering. *Canadian Geotechnical Journal*, 37, 963-986.

Freeze, R. A. (1969). The mechanism of natural ground-water recharge and discharge 1. one-dimensional, vertical, unsteady, unsaturated flow above a recharging or discharging ground-water flow system, *Water Resources Research* 5, 153 - 171.

Garg, A., Leung, A. K., & Ng, C. W. W. (2015). Comparisons of soil suction induced by evapotranspiration and transpiration of S. heptaphylla. *Canadian Geotechnical Journal*, 52(999), 1-7.

Geo-Slope . (2007), *Vadose Zone Modeling with VADOSE/W 2007*, GEO-SLOPE International Ltd, Calgary, Canada.

Gellatley, M. J., McGinnity, B. T., Barker, D. H., & Rankin, W. J. (1995). Interaction of vegetation with the LUL surface railway system. In *Vegetation and Slopes* (pp. 60-71). Oxford, England.

Glendinning, S., Loveridge, F. A., Starr-Keddle, R. E., Bransby, M. F. & Hughes, P. N. (2009). Role of vegetation in sustainability of infrastructure slopes. *Proceedings of the Institution of Civil Engineers – Engineering Sustainability*. 162, ES2, 101-110.
Glendinning, S., Hughes, P., Helm, P., Chambers, J., Mendes, J., Gunn, D. & Uhlemann, S. (2014). Construction, management and maintenance of embankments used for road and rail infrastructure: implications of weather induced pore water pressures. *Acta Geotechnica*, *9*(5), 799-816.

Greenwood, J. R., Vickers, A. W., Morgan, R. P. C., Coppin, N. J. & Norris, J. E. (2001). *Bioengineering: the Longham Wood Cutting field trial, CIRIA Project Report 81*. London: Construction Industry Research and Information Association.

Indraratna, B., Fatahi, B., & Khabbaz, H. (2006). Numerical analysis of matric suction effects of tree roots. *Proceedings of the Institution of Civil Engineers - Geotechnical Engineering*, 159, 77-90.

Leung, A. K., Garg, A., & Ng, C. W. W. (2015). Effects of plant roots on soil-water retention and induced suction in vegetated soil. *Engineering Geology*, 193, 183-197.

Li, L. J. H., Zhang, L., & Kwong, B. C. P. (2011). Field permeability at shallow depth in a compacted fill. *Proceedings of the Institution of Civil Engineers - Geotechnical Engineering*, 164, 211-221.

Loveridge, F. A., Spink, T. W., O'Brien, A. S., Briggs, K. M. & Butcher, D. (2010). The impact of climate and climate change on UK infrastructure slopes, with particular reference to southern England. *Quarterly Journal of Engineering Geology and Hydrogeology.* 43 (4), 461-472.

London Underground Ltd (2010). *Civil Engineering Technical Advice Note G-058A11*. Technical report. London Underground Ltd, London, UK.

Mualem, Y. (1976). A new model for predicting the hydraulic conductivity of unsaturated porous media. *Water Resources Research*, 12, 513-522.

Nyambayo, V. P. & Potts, D. M. (2010). Numerical simulation of evapotranspiration using a root water uptake model. *Computers and Geotechnics*, 37, 175- 186.

O'Brien, A.S., Ellis, E.A., & Russell, D. (2004). Old railway embankment fill – laboratory experiments, numerical modelling and field behaviour. In: *Advances in Geotechnical Engineering: Proceedings of the Skempton Conference*, London, Volume 2 (pp. 911-921). London: Thomas Telford.

O'Brien, A. S. (2007). Rehabilitation of urban railway – investigation, analysis, and stabilisation. *In: Proceedings of the 14th International Conference on Soil Mechanics and Geotechnical Engineering*, *Madrid,* (Cuellar, V., Dapena, E. *et al* (eds)). Millpress, Amsterdam, the Netherlands, pp. 125-143.

O'Brien, A. S. (2013) The assessment of old railway embankments – time for a change? In *Partial saturation in compacted soils: Géotechnique symposium in print* 2011, 19-32 [http://dx.doi.org/10.1680/geot.sip11.ks]

Prasad, R. (1988). A linear root water uptake model. *Journal of Hydrology*, 99, 297-306.

Rees, S. W., & Ali, N. (2006). Seasonal water uptake near trees: a numerical and experimental study. *Geomechanics and Geoengineering: An International Journal*, 1(2), 129-138.

Richards, L. A. (1931). Capillary conduction of liquids through porous mediums. *Journal of applied physics,* 1 (5), 318-333.

Ridley A. M., Dineen, K., Burland J. B. & Vaughan P. R. (2003). Soil matrix suction: some examples of its measurement and application in geotechnical engineering. *Géotechnique* 53 (2), 241-253.

Ritchie, J. T. (1972), Model for Predicting Evaporation from a Row Crop with Incomplete Cover, *Water Resources Research* 8(5), 1204 - 1212.

Rutter, A.J. and Morton, A.J., 1977. A predictive model of rainfall interception in forests. III. Sensitivity of the model to stand parameters and meteorological variables. *Journal of Applied Ecology*, pp.567-588.

Scott, J. M., Loveridge, F., & O'Brien, A. S. (2007). Influence of climate and vegetation on railway embankments. *In: Proceedings of the 14th International Conference on Soil Mechanics and Geotechnical Engineering*, *Madrid,* (Cuellar, V., Dapena, E. *et al* (eds)). Millpress, Amsterdam, the Netherlands, pp. 659-664.

Selig, E. T., & Waters, J. M. (1994). *Track geotechnology and substructure management*. Thomas Telford.

Smethurst, J. A., Briggs, K., Powrie, W., Ridley, A. and Butcher, D., (2015). Mechanical and hydrological impacts of tree removal on a clay fill railway embankment. *Géotechnique*, 65 (11), pp. 869-882.

Smethurst, J. A. (2010). Tracking changes. *Ground Engineering*. July, 12-14.

Smethurst, J. A., Clarke, D. & Powrie, W. (2006). Seasonal changes in pore water pressure in a grass covered cut slope in London Clay. *Géotechnique*, 56 (8), 523-537.

Tratch, D. J., Wilson, G. W., & Fredlund, D. G. (1995). An introduction to analytical modelling of plant transpiration for geotechnical engineers. In Proceedings of the 48th *Canadian Geotechnical Conference, Vancouver, Canada,* pp. 771-780.

Van Genuchten, M. T. (1980), A closed-form equation for predicting the hydraulic conductivity of unsaturated soils, *Soil Society of America* 44, 892 - 898.

Wilkinson, P.L., Anderson, M.G. and Lloyd, D.M., 2002. An integrated hydrological model for rain-induced landslide prediction. *Earth Surface Processes and Landforms*, 27(12), pp.1285-1297.

Wilson, G., Fredlund, D., and Barbour, S.L. (1994), `Coupled soil-atmosphere modeling for soil evaporation', *Canadian Geotechnical Journal* 31, 151 - 161.

Weather Underground (2013), Weather station isouthen6. See http://www.wunderground.com (accessed May 2013).

Table 1: Summary of soil properties used in the finite element model

Soil property	Surface clay fill	Clay fill	London Clay	Ash & ballast
Saturated hydraulic conductivity, k_{sat} (ms^{-1})	5×10^{-7}	5×10^{-8}	5×10^{-9}	1.75×10^{-5} ††
Void ratio	0.47	0.47	0.47†	0.25††
Van Genuchten constants:				
a (kPa)	30.3	30.3	125†	2.5††
θ_s	0.47	0.47	0.47†	0.25††
θ_r	0.1	0.1	0.1†	0††
m	0.13	0.13	0.15†	0.1††
n	1.15	1.15	1.18†	1.17††
Compressibility coefficient, m_v (m^2/MN)	0.05[a]	0.05[a]	0.05[a]	0.02 [d]
Thermal conductivity ($Wm^{-1}K^{-1}$)	1.79 [b]	1.79 [b]	1.79 [b]	3.4 [c]
Volumetric heat capacity ($MJ/m^3/°C$)	2.4 [c]	2.4 [c]	2.4 [c]	2.4 [c]

† van Genuchten parameters curve-fitted to data for drying London Clay (Croney, 1977)
†† Fouled Ballast (Duong *et al*., 2013)
[a] Bell (1992)
[b] Banks *et al*. (2013)
[c] Banks (2012)
[d] Selig & Waters (1994)

Table 2: Summary of weather data, time steps and root depth applied to the slopes of the finite element model within the extents of tree removal (Figure 4; for tree removal scenario). The mature tree cover boundary condition was applied beyond the extents of tree removal at all stages of the model.

Model stage	Weather data	Time step	Vegetation cover type	Root depth
Initial condition	Jan'01 - Jan'06	Days 0 - 1826	Mature trees (deep rooted)	3 m
Before tree removal	Jan'06 - Apr'07	Days 1826 - 2281	Mature trees (deep rooted)	3 m
After tree removal	Apr'07 - Apr'11	Days 2281 - 3741	Newly established scrub vegetation	0.2 m

Table 3. Summary of weather data used in the finite element model

Dates	Total potential evapotranspiration (mm)**	Total rainfall (mm)
01 Jan 2001 – 31 Dec 2001	639	654†
01 Jan 2002 –31 Dec 2002	652	624†
01 Jan 2003 – 31 Dec 2003	693	416†
01 Jan 2004 – 31 Dec 2004	660	526†
01 Jan 2005 – 31 Dec 2005	630	477†
01 Jan 2006 – 31 Dec 2006	691	532*
01 Jan 2007 – 31 Dec 2007	676	570*
01 Jan 2008 – 31 Dec 2008	632	607*
01 Jan 2009 – 31 Dec 2009	639	592*
01 Jan 2010 – 31 Dec 2010	664	640*
01 Jan 2011 – 31 Mar 2011	59	159*

**Calculated using the Penman-Monteith equation (Allen *et al*., 1994) and weather data measured at Shoeburyness, Essex (Weather Underground, 2013)

† Measured at Shoeburyness, Essex (Weather Underground, 2013)

* Measured at Hawkwell, Essex (Smethurst *et al*., 2015)

Figures

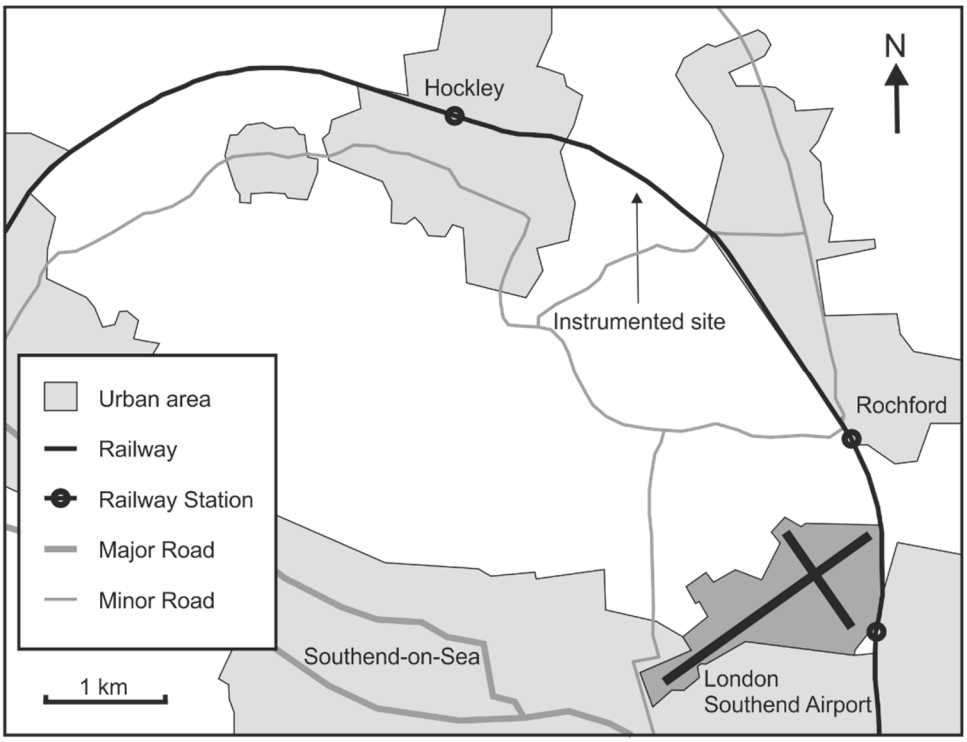

(a)

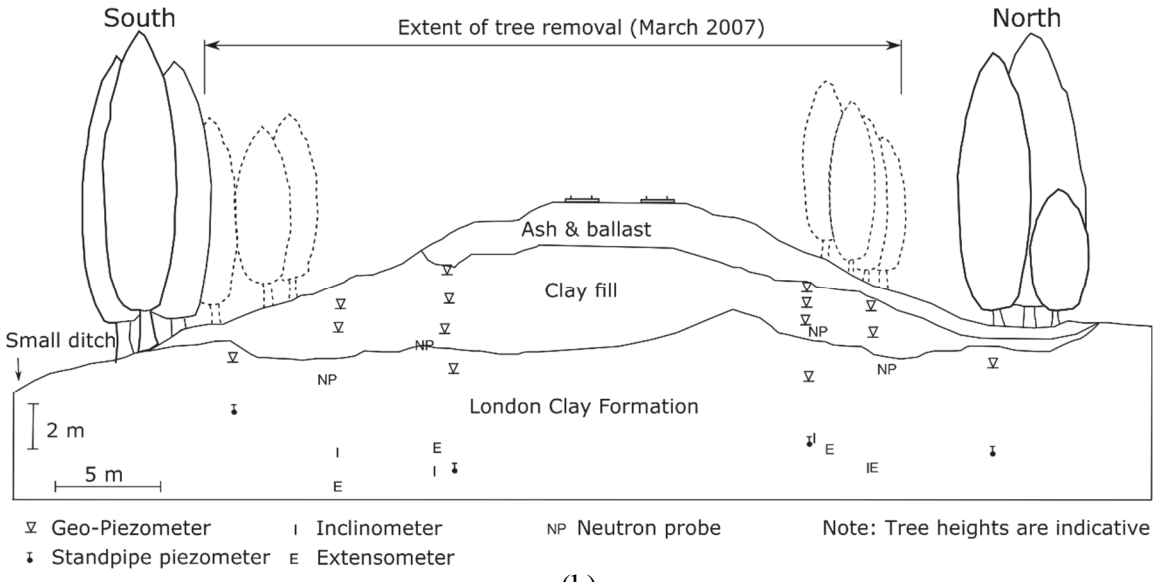

(b)

Fig 1: (a) Location of the instrumented site; (b) The instrumented section of Hawkwell embankment (From Smethurst *et al.*, 2015). Note that the symbols mark the maximum extent of installation and that the tree location, form and height are not to scale.

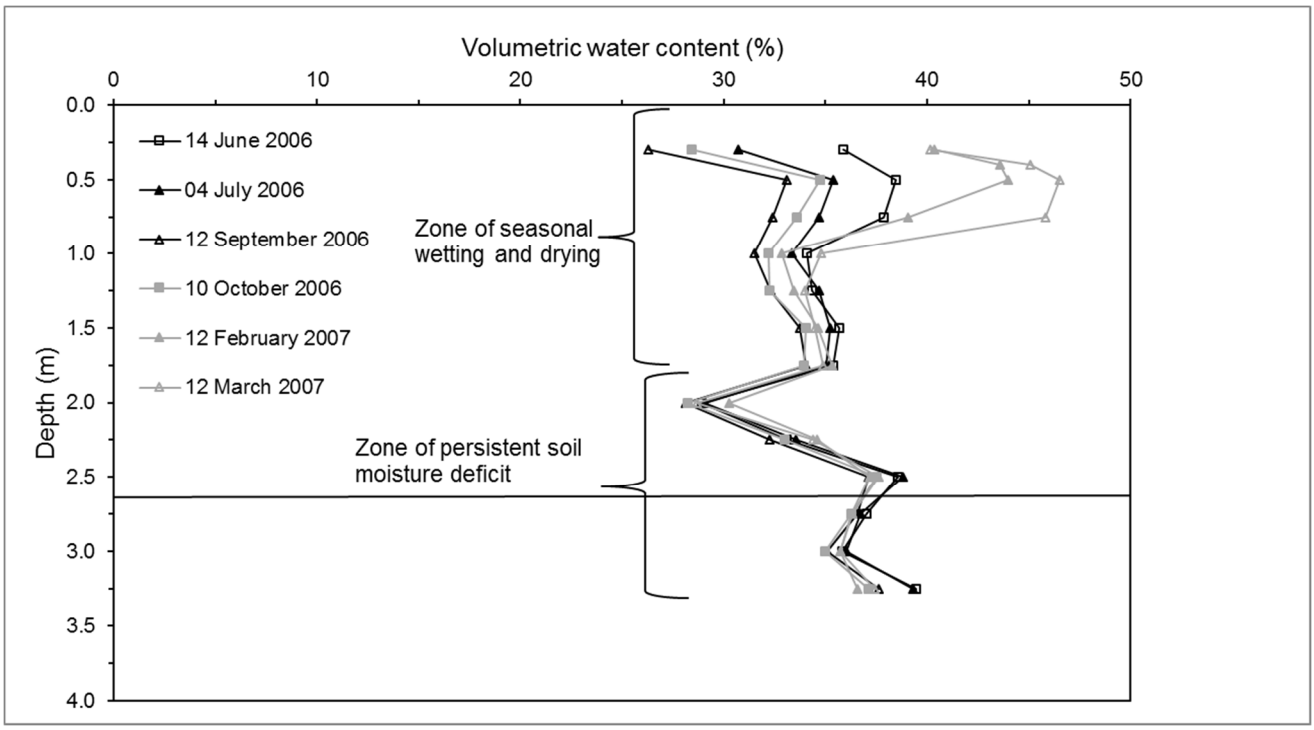

(a)

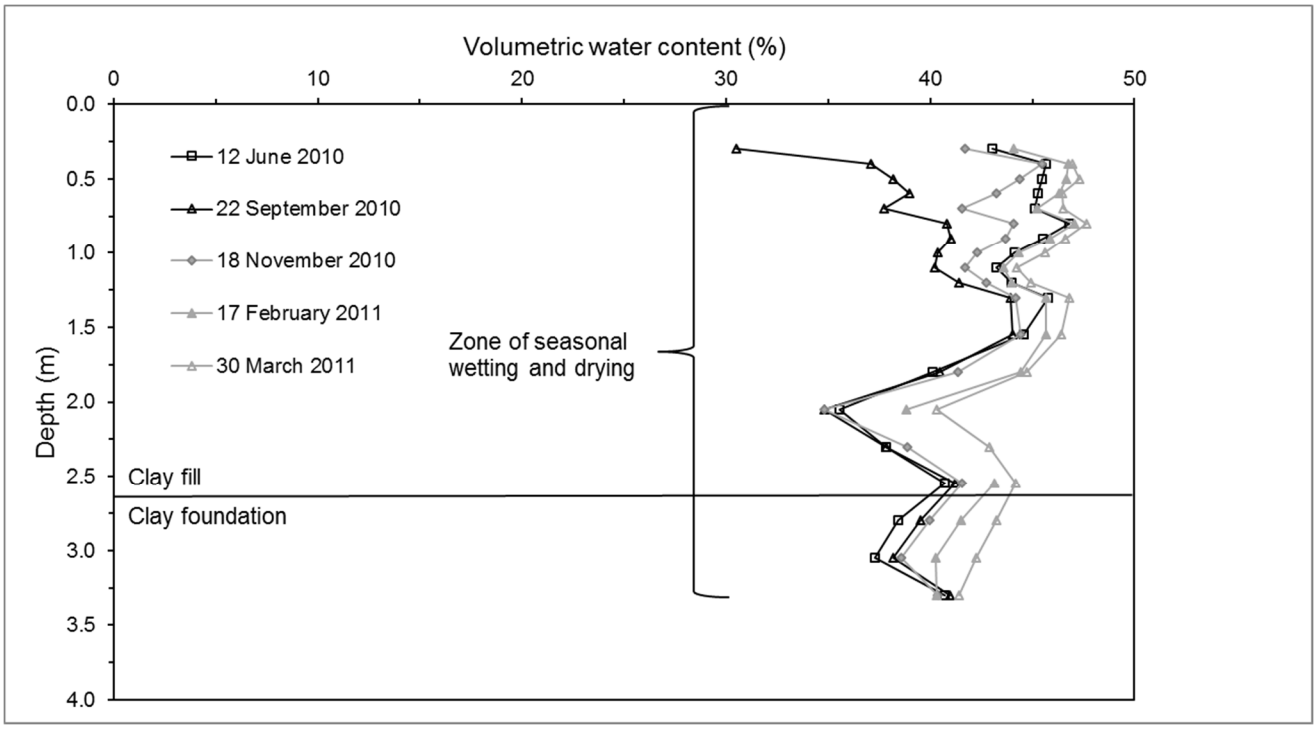

(b)

Figure 2: Measured volumetric water content variation at the middle of the south embankment slope (a) Prior to tree removal (b) Four years after tree removal

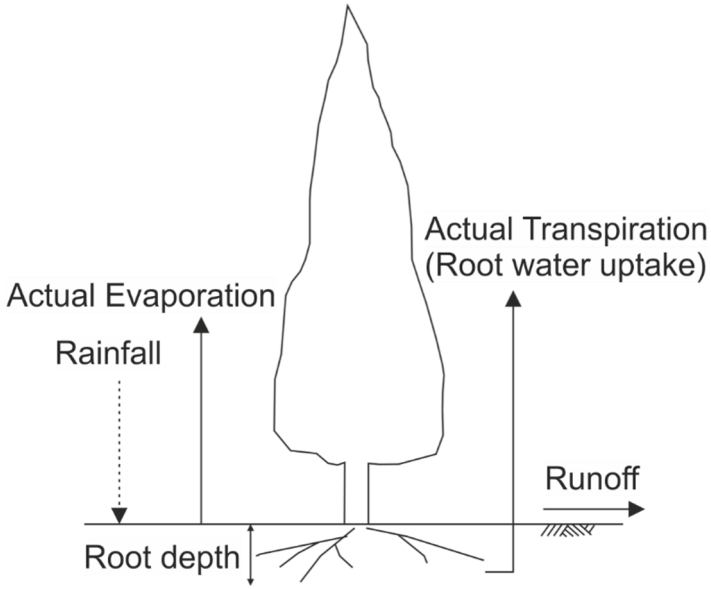

Figure 3: The surface water balance with root water uptake

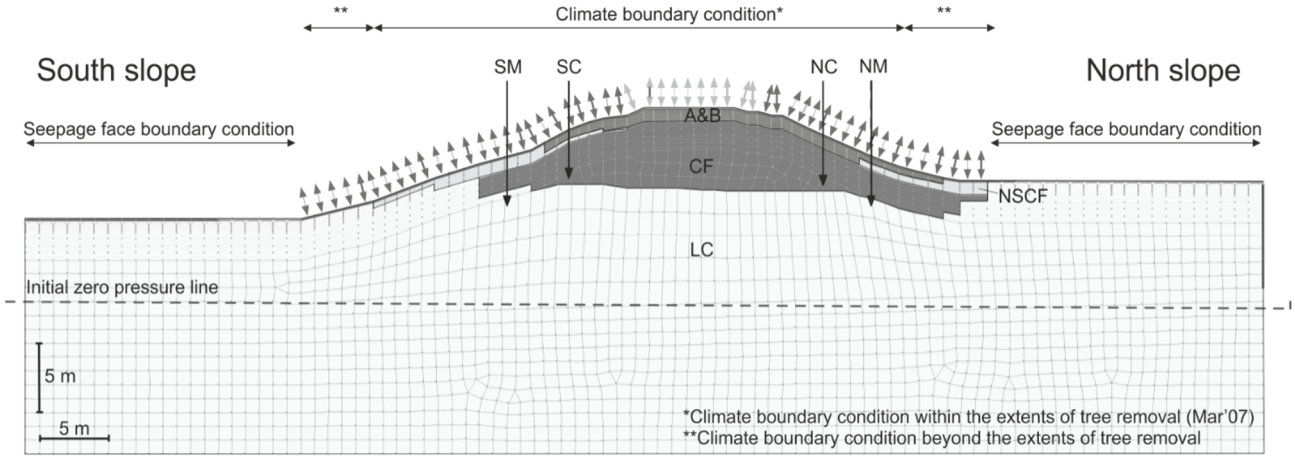

Figure 4: Finite element model of Hawkwell embankment showing geometry, soil layers and the instrumentation and monitoring locations. Instrumentation locations at the south midslope (SM), south crest (SC), north crest (NC) and north midslope (NM) are shown. London Clay Formation (LC), clay fill (CF), near surface clay fill (NSCF) and ash & ballast (A&B) soil layers are shown. The boundary condition parameters are shown in Table 2.

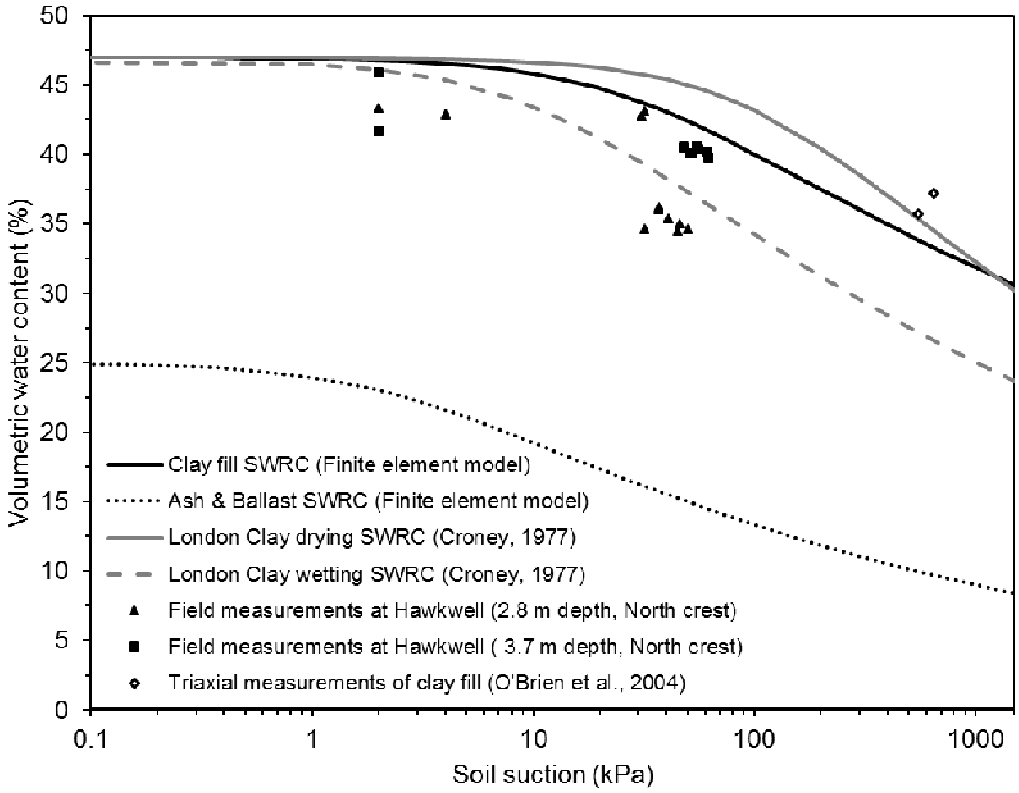

Figure 5: Comparison of pore water pressure and volumetric water content measurements at Hawkwell embankment with triaxial measurements of clay fill (O'Brien *et al*., 2004) and with soil water retention curves (SWRC's) for the wetting and drying of London Clay (Croney, 1977)

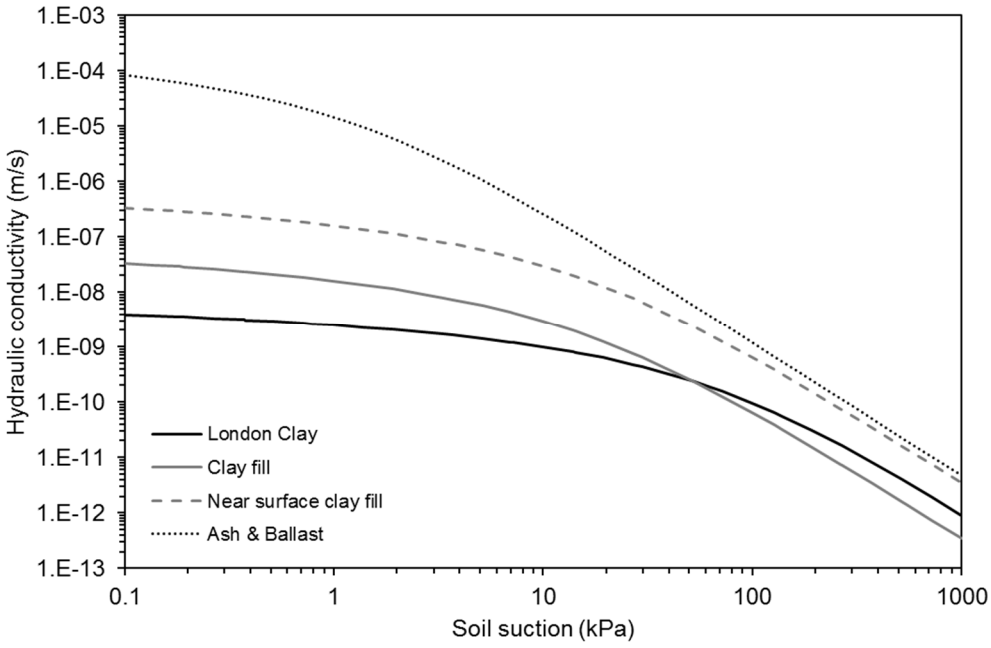

Figure 6: Curves showing the reduction of hydraulic conductivity with increasing soil for London Clay, clay fill, surface clay fill and the ash and ballast soil layers.

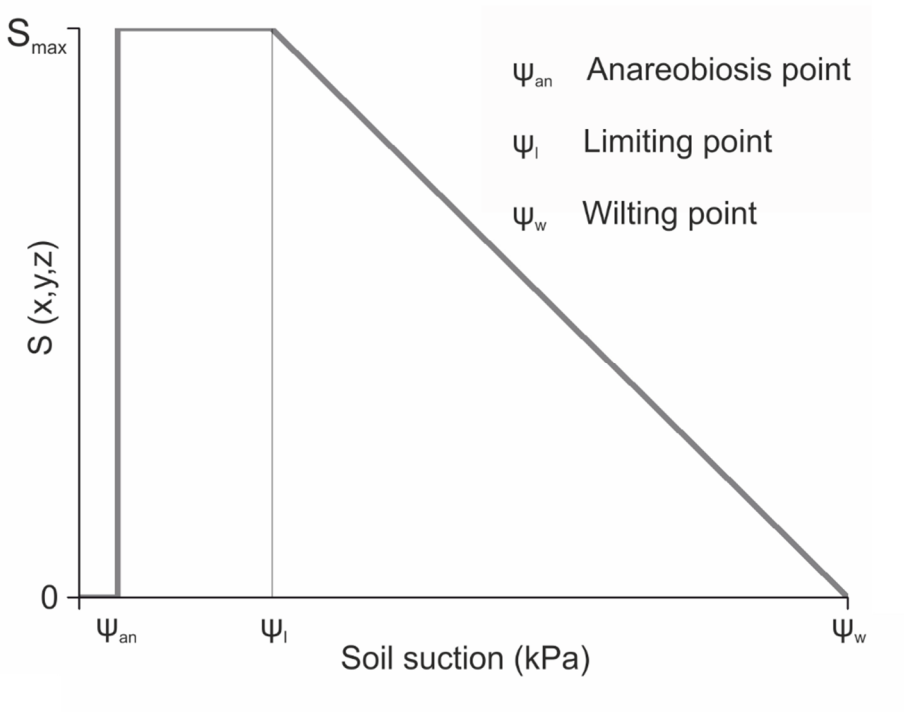

Figure 7: Reduction coefficient for root water uptake rate (S) as a function of soil suction (kPa). Water uptake is zero at suctions below the anareobiosis point (oxygen deficiency) and above the wilting point (Adapted from Feddes *et al*. 1978).

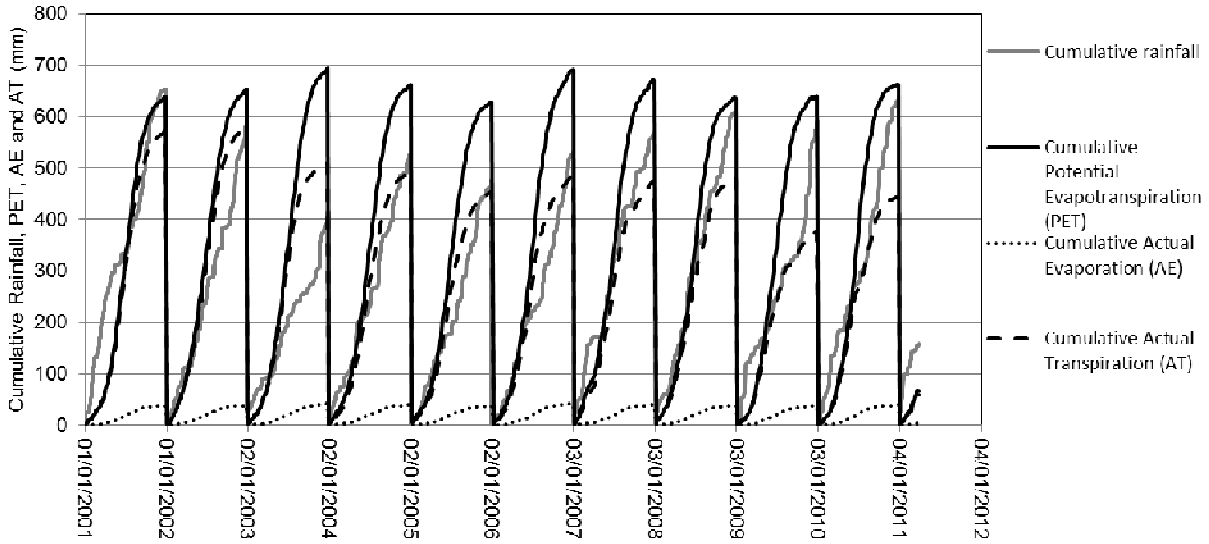

Figure 8: Cumulative rainfall, Potential Evapotranspiration (PET), Actual Evaporation (AE) and Actual Transpiration (AT) applied to the boundary condition of the finite element model simulating tree removal in March 2007.

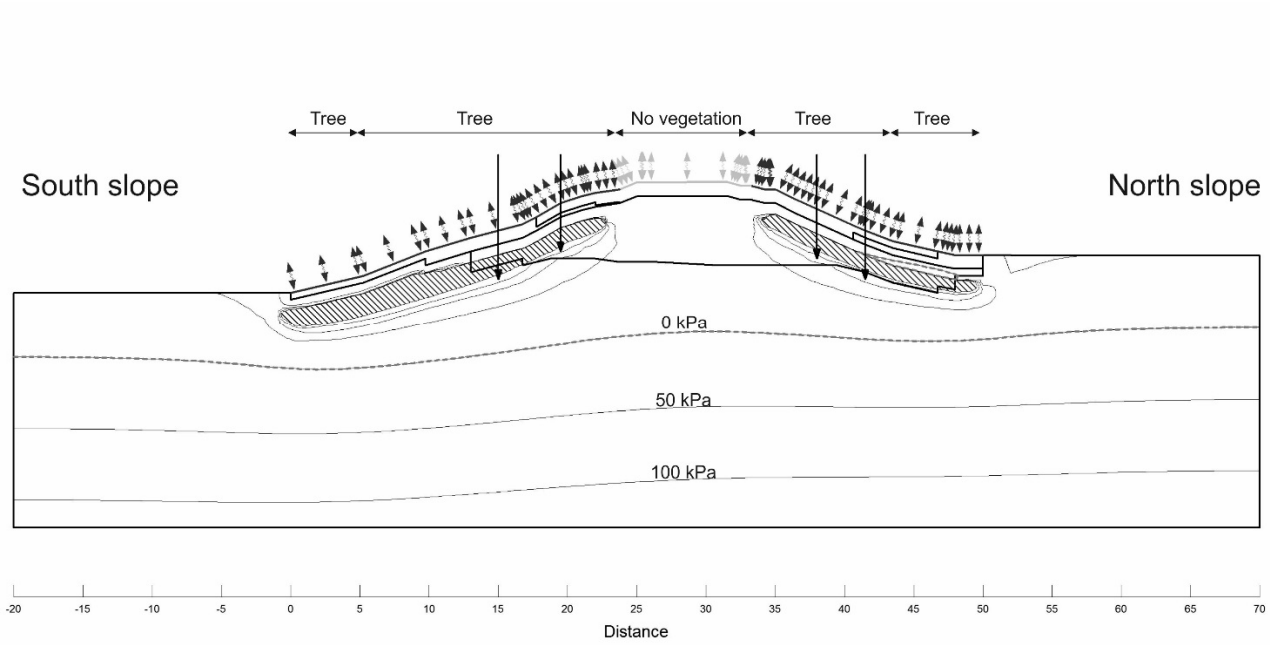

Figure 9: Contour plot of pore water pressure at the end of winter in March 2007, before tree removal. Suctions greater than 200 kPa are shown as hatched for clarity.

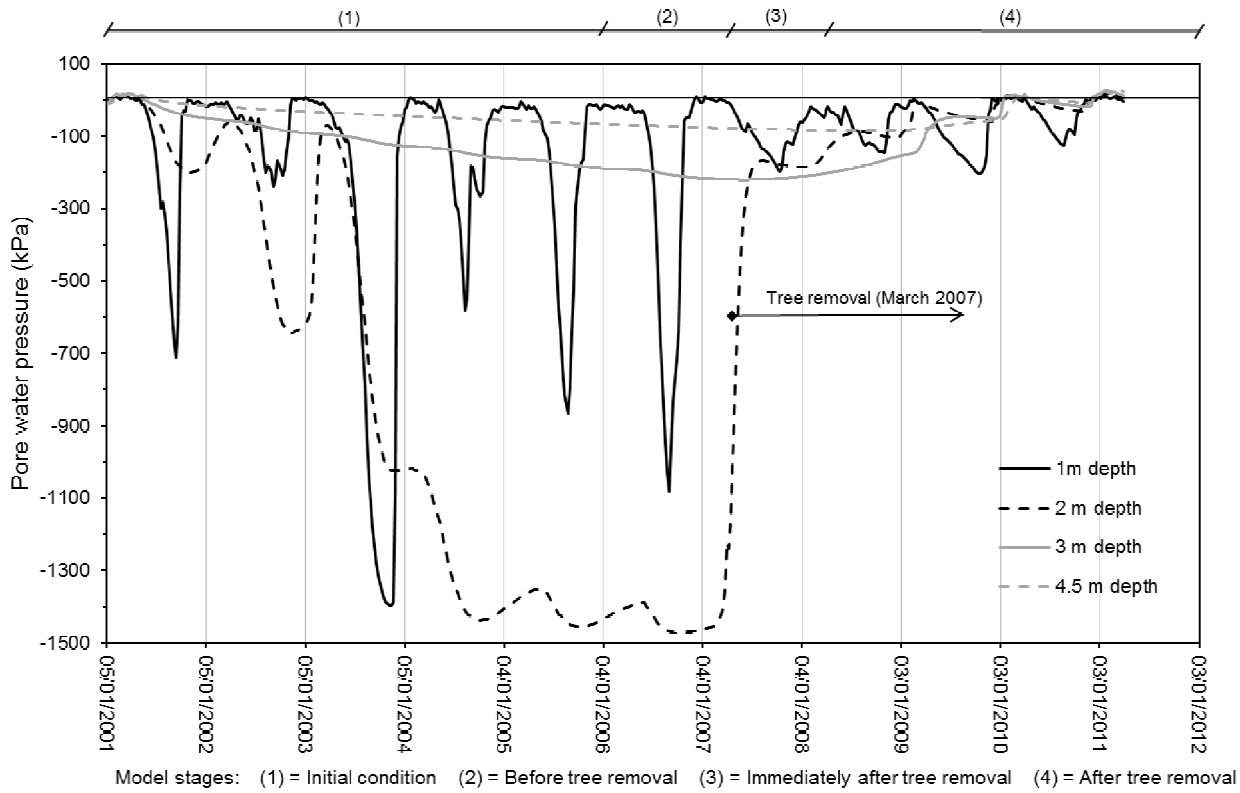

(a)

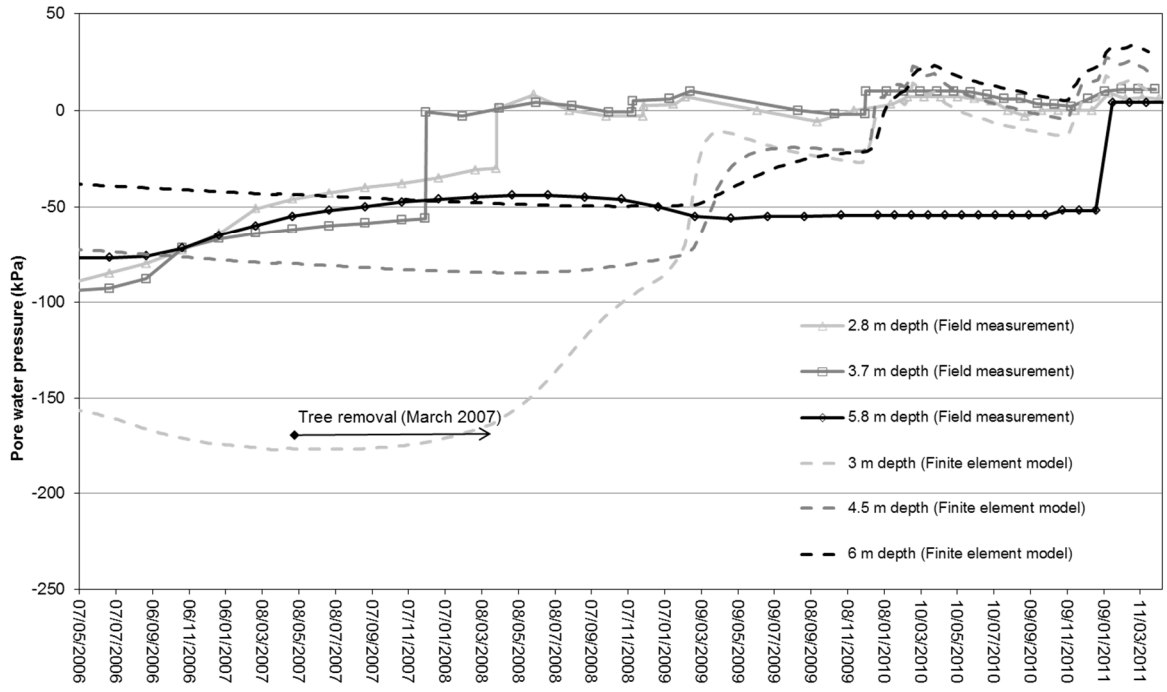

(b)

Figure 10: (a) Pore water pressure variation within the finite element model at the midslope of the south facing embankment slope; (b) Comparison between the finite element model and field measurements of pore water pressure at the crest of the north facing embankment slope

(field measurements adapted from Smethurst *et al*., 2015)

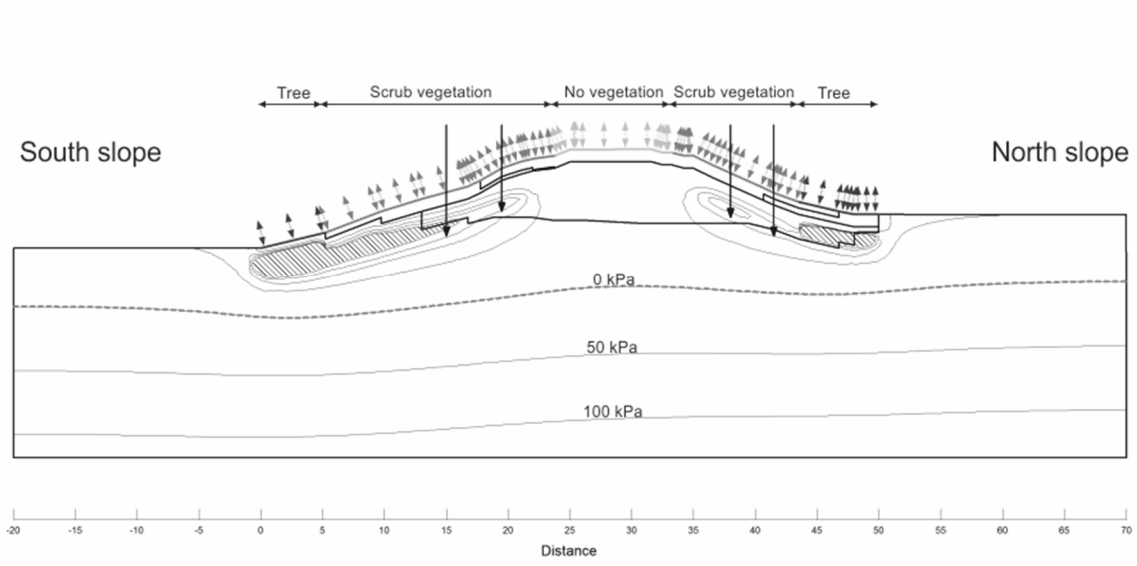

(a)

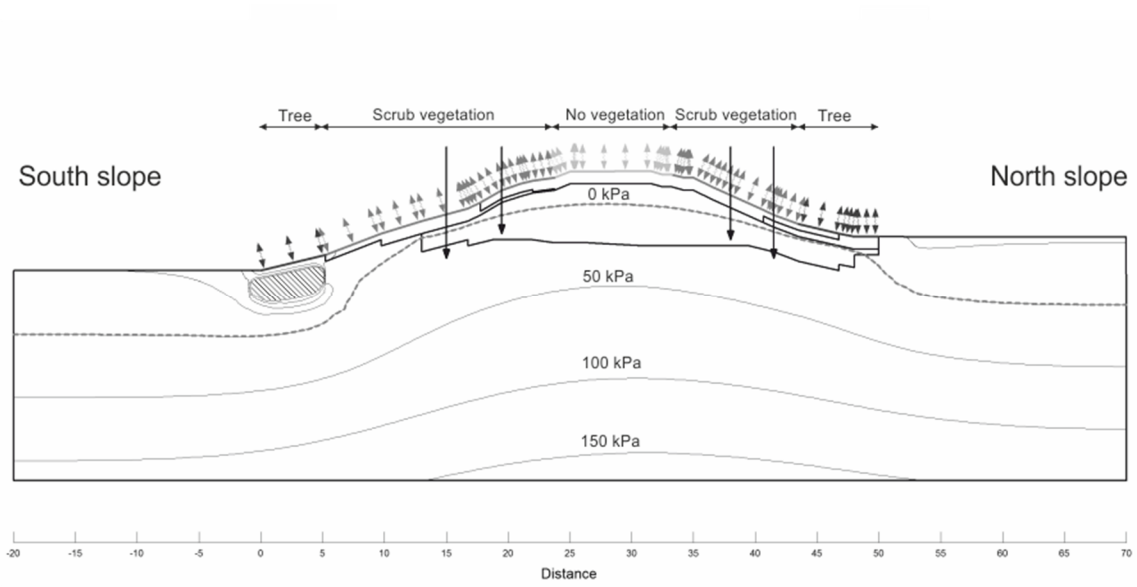

(b)

Figure 11: Contour plot of pore water pressure at the end of winter in a) March 2008, one year after tree removal b) March 2011, four years after tree removal. Suctions greater than 200 kPa are shown as hatched for clarity.

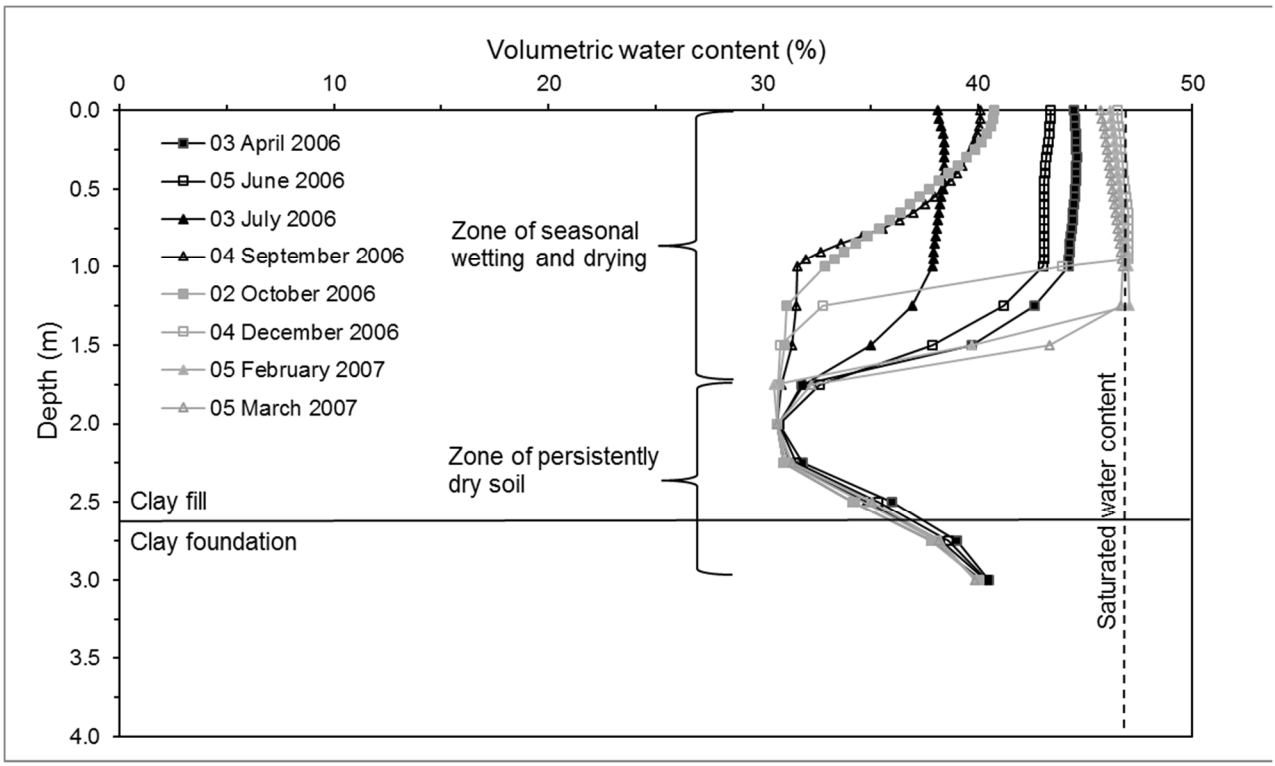

(a)

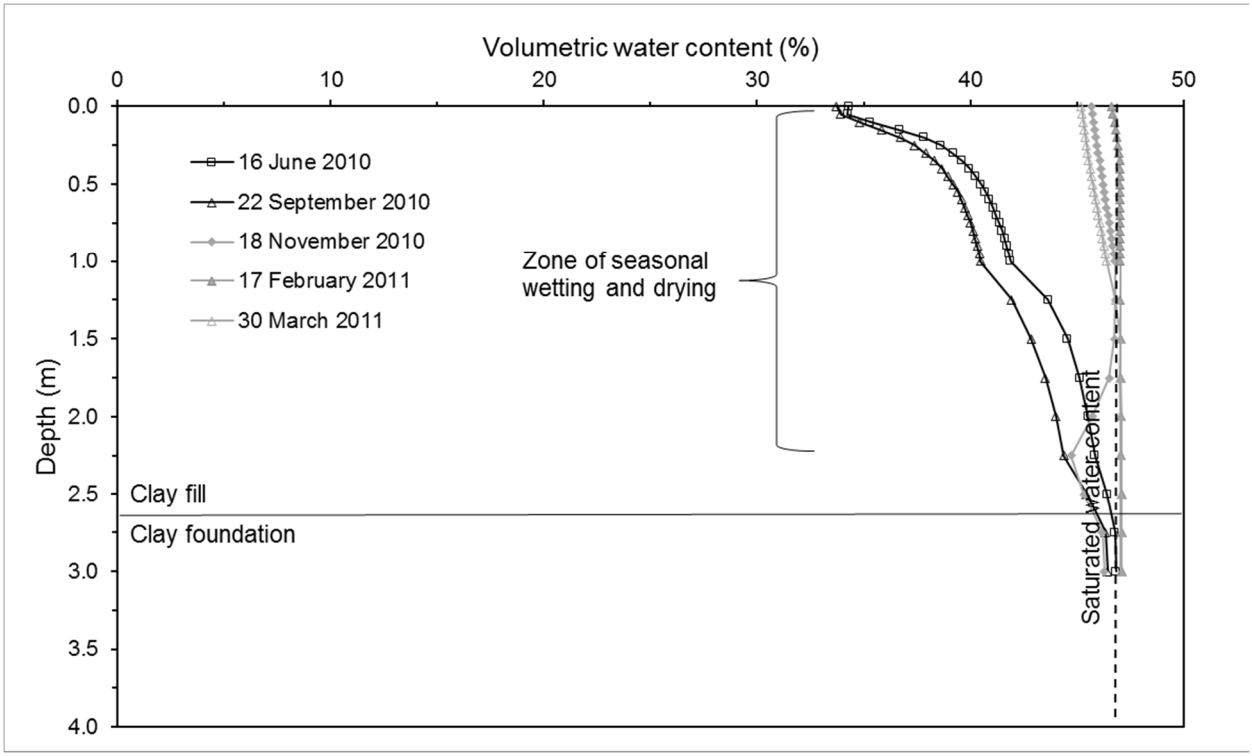

(b)

Figure 12: Volumetric water content variation at the middle of the south embankment slope calculated using the finite element model (a) Prior to tree removal (b) Four years after tree removal

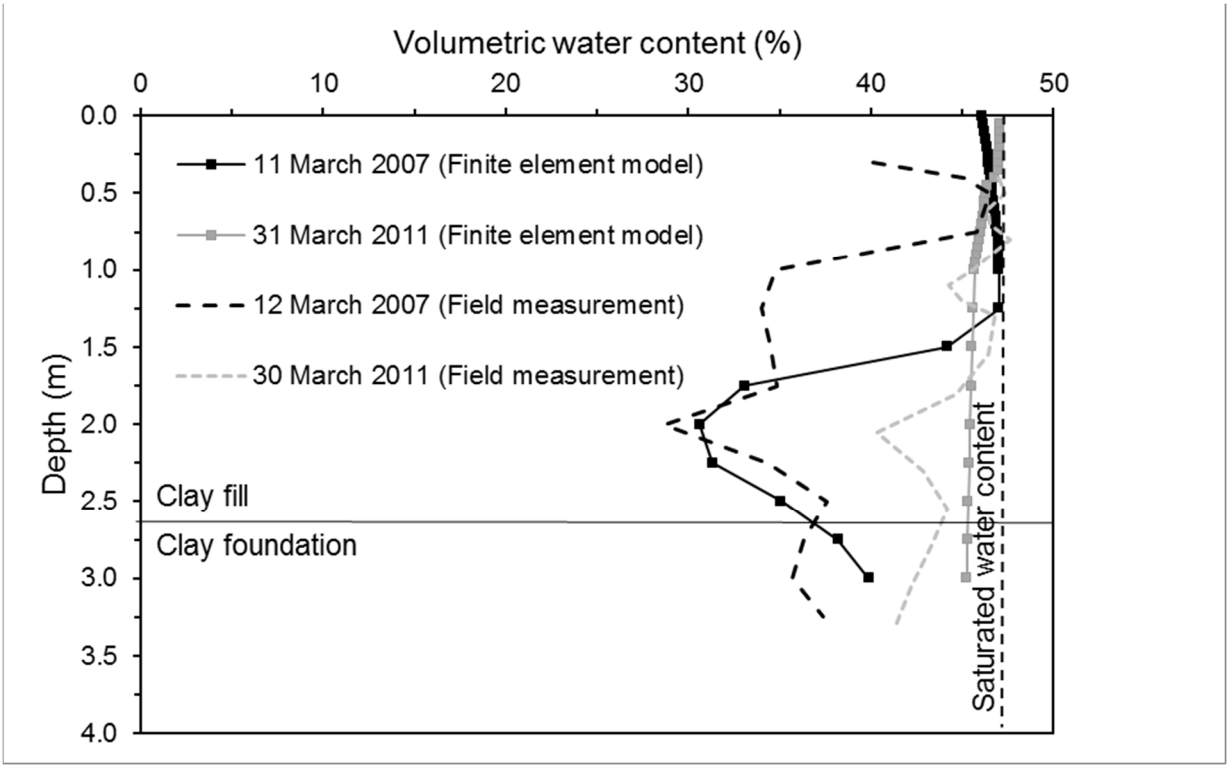

(a)

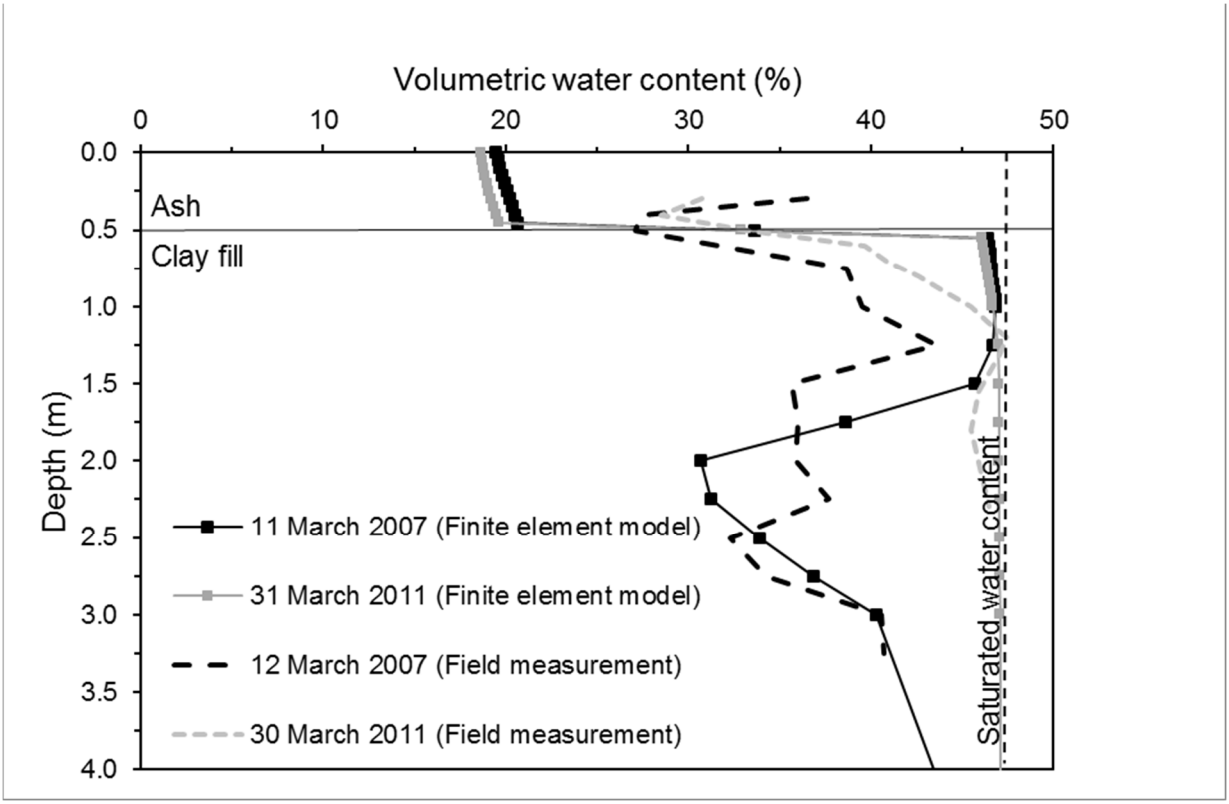

(b)

Figure 13: Volumetric water content calculated within the finite element model before and after tree removal at (a) the middle of the south facing slope (b) the middle of the north facing slope. Field measurements of volumetric water content are shown for comparison.

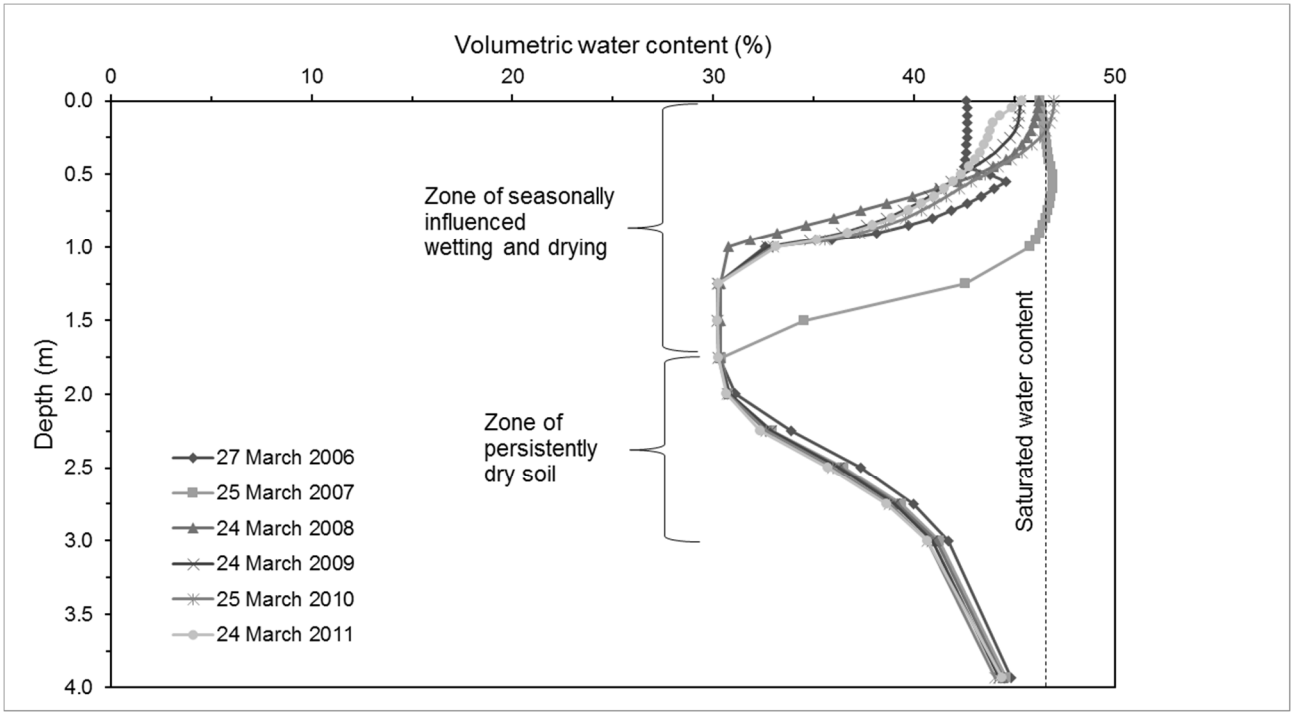

(a)

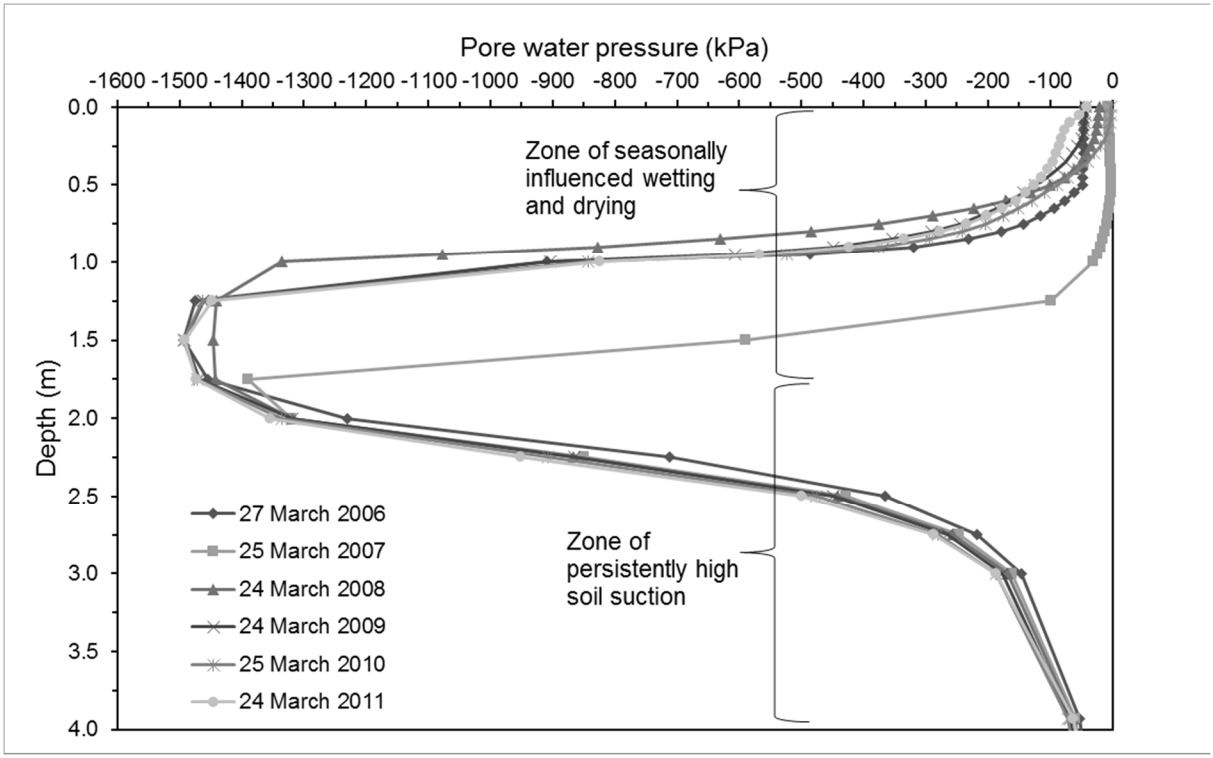

(b)

Figure 14: (a) Volumetric water content and (b) pore water pressure, calculated within the finite element model for the end of winter (March) between 2006 and 2011 at the tree covered toe of the south facing slope.

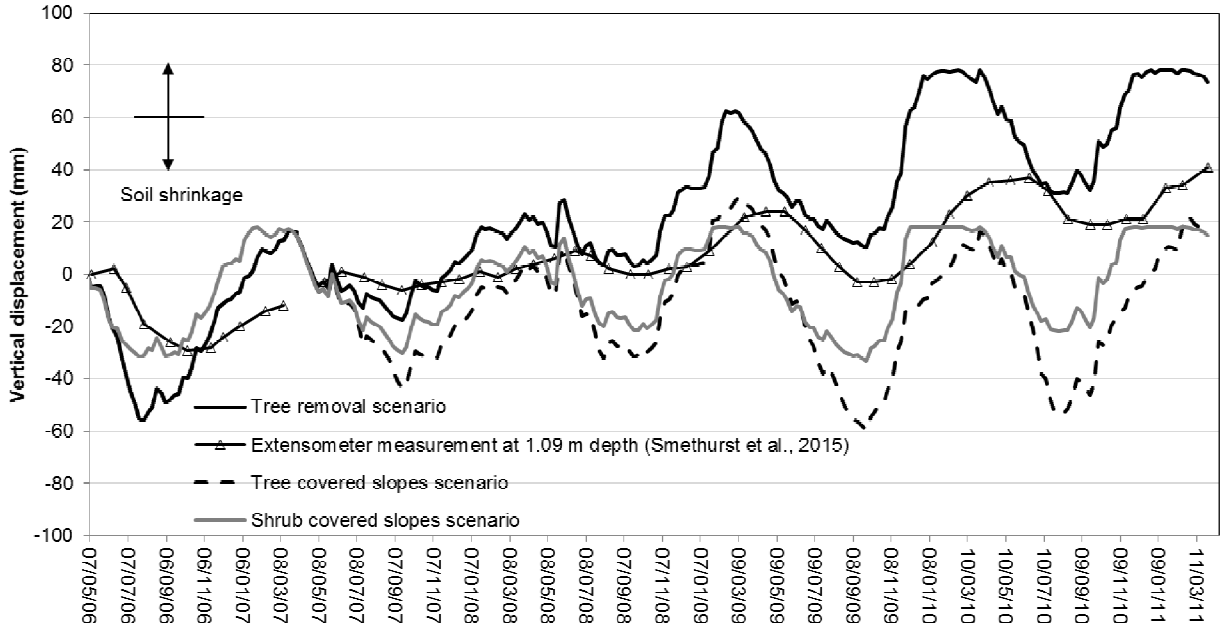

Figure 15. Vertical displacement within the clay fill layer (0m – 3m depth) at the south midslope calculated from volumetric water within the finite element model. Results for vegetation cover scenarios with a) tree removal in March 2007 b) tree covered slopes c) shrub covered slopes are shown. Extensometer measurements from Smethurst *et al*., (2015) are shown.

Appendix

Moisture and heat flow

The two dimensional slope was numerically modelled in Vadose/w (Geo-Slope ,2007), which uses equations [A1] and [A2] to govern the coupled moisture and heat flow in soil respectively:

$$\frac{1}{\rho}\frac{\partial}{\partial x}\left(D_v\frac{\partial P_v}{\partial x}\right)+\frac{1}{\rho}\frac{\partial}{\partial y}\left(D_v\frac{\partial P_v}{\partial y}\right)+\frac{\partial}{\partial x}\left(k_x\frac{\partial[P/\rho g]}{\partial x}\right)+\frac{\partial}{\partial y}\left(k_y\frac{\partial[(P/\rho g)+y]}{\partial y}\right)+Q=\lambda\frac{\partial P}{\partial t} \quad [A1]$$

$$L_v\frac{\partial}{\partial x}\left(D_v\frac{\partial P_v}{\partial x}\right)+L_v\frac{\partial}{\partial y}\left(D_v\frac{\partial P_v}{\partial y}\right)+\frac{\partial}{\partial x}\left(k_{tx}\frac{\partial T}{\partial x}\right)+\frac{\partial}{\partial y}\left(k_{ty}\frac{\partial T}{\partial y}\right)+Q_t+\rho cV_x\frac{\partial T}{\partial x}+\rho cV_y\frac{\partial T}{\partial y}=\lambda_t\frac{\partial T}{\partial t} \quad [A2]$$

where ρ is the water density, D_v is the vapour diffusivity coefficient, L_v is the latent heat of vaporisation, P_v is the vapour pressure of soil moisture, k is the saturated hydraulic conductivity, k_t is the thermal conductivity, y is the elevation head, t is time, P is the water pressure, g is the acceleration due to gravity, Q is the applied hydraulic boundary flux, Q_t is the applied thermal boundary flux, λ is the slope of the volumetric water content function in the soil water retention curve, λ_t is the volumetric heat capacity of the soil, c is the specific heat capacity of the fluid and V is the Darcy's flow velocity.

The moisture and heat flow equations are coupled using the relative humidity equation proposed by Edlefsen and Anderson (1943) [A3]:

$$P_{v.soil}=h_r\,P_{v.sat.soil}=P_{v.sat.soil}\,e^{\psi g\omega_w/\gamma_w R(273.15+T_s)} \quad [A3]$$

where $P_{v.soil}$ is the vapour pressure at the soil surface, h_r is the relative humidity at the soil surface, $P_{v.sat.soil}$ is the saturated vapour pressure at the soil surface, ψ is the total suction, ω_w is the molecular weight of water, γ_w is the unit weight of water, R is the universal gas constant and T_s is the temperature at the soil surface.

Boundary conditions

Potential evapotranspiration (PET) was calculated using the Penman-Monteith equation (Allen *et al.*, 1994) for a grass crop (albedo of 0.23 and canopy surface resistance of 70 s m^{-1}) and the daily weather data summarised in Table 3.

$$PET=\frac{0.408(R_n-G)+\gamma\frac{900}{T+273}u_2(P_{v.sat.air}-P_{v.air})}{\Delta+\gamma(1+0.34u_2)}$$

[A4]

where γ is the psychrometric constant, T is the daily air temperature at 2 m height, R_n is net radiation at the crop surface, G is the soil heat flux density, u_2 is the wind speed at 2 m height, Δ is the slope of the saturation vapour curve, $P_{v.sat.air}$ is the saturated vapour pressure of the air above the soil surface and $P_{v.air}$ is the actual vapour pressure of the air above the soil surface.

Evaporation is calculated for an unsaturated soil, where suctions limit the evaporation rate using the Penman-Wilson formulation (Wilson *et al*., 1994):

$$E = PET\left[\frac{h_{r-}(P_{v.sat.air}/P_{v.sat.soil})h_a}{1-(P_{v.sat.air}/P_{v.sat.soil})h_a}\right]$$

[A5]

where PET is the potential evapotranspiration (Table 3), h_r is the relative humidity at the soil surface, h_a is the relative humidity of the air above the soil surface, $P_{v.sat.soil}$ is the saturated vapour pressure at the soil surface and $P_{v.sat.air}$ is the saturated vapour pressure of the air above the soil surface.

The soil evaporative flux at the ground surface (Equation A4) is modified to separate actual evaporation (AE) and potential transpiration (PT) using equations [A6] and [A7]. Field measurements were unavailable, but Rutter & Morton (1977) suggest a LAI of 6.0-6.5 for Oak trees in the UK. A constant Leaf Area Index (LAI) of 2.7 (the maximum allowable LAI using Vadose/w) was assumed in the model to represent full leaf cover, hence simplifying the AE and PT equations as shown.

$$AE = E\left[1-\left(-0.21+0.7\sqrt{LAI}\right)\right] = E(0.06)$$

[A6]

$$PT = E\left(-0.21+0.7\sqrt{LAI}\right) = E(0.94)$$

[A7]

The potential transpiration (PT) in unsaturated soil is further reduced using a reduction coefficient (S; Figure 8). Actual nodal transpiration (AT) is defined as

$$AT = (PRU)(S)$$

[A8]

where Plant Root Uptake (PRU) is defined as

$$PRU = \frac{2PT}{R_T}\left(1-\frac{R_n}{R_T}\right)A_N$$

[A9]

where R_T is the root zone depth (Table 2), R_n is the depth of the node and A_n is the nodal contributing area of the node. A_n is assumed to be linear with depth in the Hawkwell model.

References

Allen, R. K., Smith, M., Perrier, A., & Pereira, L. S. (1994). An update for the calculation of Reference Evapotranspiration. *ICID Bulletin*, 43(2),35-92.

Edlefsen, N. E., & Anderson, A. B. C. (1943). Thermodynamics of soil moisture. *Hilgardia* , 15(2).

Geo-Slope . (2007), *Vadose Zone Modeling with VADOSE/W 2007*, GEO-SLOPE International Ltd, Calgary, Canada.

Rutter, A.J. and Morton, A.J., 1977. A predictive model of rainfall interception in forests. III. Sensitivity of the model to stand parameters and meteorological variables. *Journal of Applied Ecology*, pp.567-588.

Wilson, G., Fredlund, D. and Barbour, S. (1994). Coupled soil-atmosphere modeling for soil evaporation, *Canadian Geotechnical Journal* 31, 151 - 161.